Mathematical Modelling and Computational Dynamics of Quasi-Lockdown Control of COVID-19 Pandemic in Akwa Ibom State, Nigeria

Abstract

Assessing the efficacy of a local control strategy, implemented to curtail the spread of COVID-19 has become obligatory for safeguarding policy makers in preparations to combat the so-called long covid. This research used a deterministic SEIAHR-model, incorporating a logistic function to investigates the effect of quasi-lockdown policy during re-emergence of the infectious disease. The notion of uniform convergence and fixed point theory were used to established positive invariant region, ultimate boundedness, and existence of unique solution of the model. Nonlinear dynamical behaviours of the model such as stability and oscillating flows occurred at the disease free, and endemic equilibrium points. Using centre manifold theory, a transcritical bifurcation with hysteresis effect were established, when the quasi-lockdown parameter was used as a control parameter. A forward sensitivity analysis was conducted to unfold parameters that contributed significantly towards the spread and control of the infection. These parameters were estimated and fitted using least square technique, comparative to the observed real datasets adapted from the Nigeria Centre for Disease and Control (NCDC). The polynomial regression model fitted the observed datasets with an average coefficients of determination; $R^2 = 0.94$. Simulations and phase space diagrams with the help of maple16, were used to validate the theoretic results. Epidemiologically, the model demonstrated that quasi-lockdown policy was necessarily a strategic policy to curbing the spread of the infection, but not sufficient to eradicate the disease as the disease persisted endemically. It was showed that the basic reproduction number of the infection was below the critical threshold $R_0 \leq 1$, when lockdown policy was enforced strictly, but otherwise on relaxation of the lockdown policy. In the same vein, a relaxation of the quasi-lockdown policy leads to increase in the susceptibility of the populace as the infection risk ratio increases. Similarly, the model predicted that a pre-mature lifting of the lockdown policy could have leads to high infectivity on the susceptible class and disastrous to health-being of the citizens.

Key words: COVID-19 pandemic, Computational dynamics, Mathematical modelling, and Quasi-Lockdown policy.

1.0 Introduction

Emergence and re-emergence of infectious diseases such as corona viruses are integral parts of the natural ecological system. Coronaviruses (CoVs) are lethal zoonotic viruses, which belong to nidovirales order, coronaviridae family, and coronavirinae subfamily. They are classified into five genera, namely alpha-coronavirus, beta-corona virus, gamma-corona virus, delta-corona virus and omicron-corona virus, by phylogenetic analyses and genomic relationships. Major evolutional model shows that CoVs of each genus are found in diverse animal species including horses, bats, cows, pigs, dogs, cats, birds, and ferrets. They are highly pathogenic in nature, forming the etiological agent of diseases in humans, ranging from common cold to severe illnesses such as Middle East Respiratory Syndrome (MERS-COVs) and Severe Acute Respiratory Syndrome (SARS-COVs), enteric, hepatitic, renal, neurological, and other diseases [28, 16]. Recently, an infectious pathogen of severe acute respiratory syndrome corona virus-2 (SARS-COV-2), had emerged in Wuhan of China, and abides no global

border in 2019 termed as COVID-19. It was a viral infection that affected breathing and blockage of the nostrils, throat, bronchi and lungs. The incubation period of COVID-19 has been approximated to have a mean, median, and mode of 7.83, 7, and 5 days, and, in 12.5% of cases, more than two weeks [32]. It was characterized by sudden onset of high fever, aching muscles, headache, kidney failure, severe malaise, non-productive cough, sore throat,rhinitis, pneumonia, decrease in leukocyte counts, cytokine storm, and sudden death in severe cases. The virus was mainly transmitted easily from person to person via droplets and small particles produced when infected people cough or sneeze. SARS-COV-2 virus tends to spread rapidly and has become a seasonal epidemics. It new strain considered as corona virus (COVID-19) has been contagious and killed more than 6.9 million people with co-morbidity.
The recent advancement in biomedical technologies had initiated reliable detective and diagnostic methods of this plague. Also, early diagnostic intervention could served as a prompt management of the pandemic as well as control measures to curtail the serial and generational spread of the disease. Susceptible and exposed individuals to the virus were diagnosed of SARS-CoV-2 infection through the process of collecting various specimens, including nasopharyngeal and oropharyngeal swabs, nasopharyngeal and oropharyngeal aspirates, bronchoalveolar lavage, sputum, tracheal aspirates, and blood sample. Specimens can be stored at 4^0C for up to seventy two (72) hours after sample collection and may be stored at -70^0C for longer periods of time. Numerous techniques deployed for diagnostic purposes of COVID-19 was expounded in [29, 30, 9, 6], but these techniques have distinctive disadvantages. They discussed extensively the efficacy of diagnostic techniques in both clinical and research paradigms to include; rapid antigen/antibody tests, computed tomography imaging, immunoenzymatic serological tests, integrated molecular diagnostic based on Reverse Transcription Polymerase Chain Reaction(RT-PCR). Currently, real-time quantitative reverse transcription-PCR (rqRT-PCR) has become popular for COVID-19 diagnosis because it has a high specificity, simple quantitative analysis, and higher sensitivity comparative to the routine RT-PCR. Apart from these conventional methods, other techniques, including isothermal nucleic acid amplification techniques, clustered regularly interspaced short palindromic repeats (CRISPR)-based tests or digital PCR methods are currently used in research contexts or are awaiting approval for diagnostic use by competent authorities [26]. Inspite the declaration of COVID-19 as a "public health emergency of international concern" on January 30th, 2020 by World Health Organization (WHO), the reemergence of a new variant of SARS-COV2 "omicron-COVID-19" as reported by Network for Genomics Surveillance in South Africa breeds new challenges [27]. Consequently, the member states of WHO(2022) lunched an Intergovernmental Negotiating Body (INB) to seeking data-driven scientific reports, health surveillance, preventive and optimal control strategies of COVID-19 as the instrument for further awareness, preparedness and response. In the pursuits by INB, they drafted conceptual zero draft [19], seeking a systematic and comprehensive meta-review by many stakeholders which can facilitate the development of a new international legal instrument and obligation to safeguard against pandemic threats in the future. Although, in May $5^thMay, 2023$,the emergency committee of COVID-19 met, through the head of the United Nation (UN), the World Health Organization (WHO) has declared "with great hope" an end to COVID-19 as a public health emergency, stressing that it does not mean the disease is no longer a global threat. Thus, it could be pertinent to carry a study towards identifying the optimal control policies of the infectious disease, and determine a comprehensive cost effective strategy to safeguards the threat and mitigation of the so called long covid pandemic[3].

In Nigeria, the index case of the virus appeared on the $20^thFebruary, 2020$ in Lagos, as announced by the Nigeria Centre for Disease and Control (NCDC), and had since spreaded sporadically to other parts of the Federation including Akwa Ibom State[2, 21]. This propelled the government to take devastating measures such as the declaration of a total lockdown; closure of schools and business, including restriction of international and local travelling in the country. The pandemic reaches it epic in August, 2022 in Nigeria between week 35-36, before declining, without any death case reported in 2023. The bi-weekly epidemiologoical reports of the NCDC, as that $26^thFebruary, 2023$ show a cumulative active infected cases of 266,313 and 3,155 deaths (case confirmed fatality rate (CFR) of

1.2%) in the country. On the other hand, in Akwa Ibom state a total of 5010 confirmed case with death cases of 44 has been reported by NCDC since the outbreak of the pandemic. The first wave of COVID-19 in Akwa Ibom State witnessed the adoption of some strategic programmes to curtail the spread of the infection such as embacking on Flexible Educational Programmes(FEPs)[11, 12, 25]. This entails the synchronous and synchronous learning platforms for school children restricted by closure of schools, distance learning programmes and public health sensitization campaigns on the use of non-pharmaceutical interventions. Personal Protective Measures (PPMs) used were (a) avoiding contagious people of related symptoms, and complete social distancing(i.e., being at 2m in proximity to susceptible individuals), (b) washing of hands for at least 20 seconds, (c) using of sanitizers with at least 60% of alcohol, (d) disinfecting surfaces, and frequently touched objects, and (e) isolation of suspected infected individuals. As part of the use of Personal Protective Measures (PPMs), the government recommended and provided personal protective equipment such as use of face masks, use of hand gloves with personal protective clothing by healthcare workers while giving care to COVID-19 patients and other response mechanisms [22].

In the long run, therapeutic interventions, treatments and vaccinations became common through effort of scientific and biomedical researches. Different pharmaceuticals passed ethically approved clinical trials under the Monitored Emergency Use of Unregistered Interventions System (MEURI), with strict supervision [23, 13]. Inspite of human immune activators to reduce the viral loads, drugs were utilized to moderate the prevalence, virulence, and molecular evolution rate of the infection. Several investigatory drugs and immune modulator drugs such as chloroquine, nitazoxanide, and ribavirin in combination of PEGylated interferon alfa-2a and -2b have shown inhibitory action against SARS-CoV-2 infection[18], as shown in figure 1 below

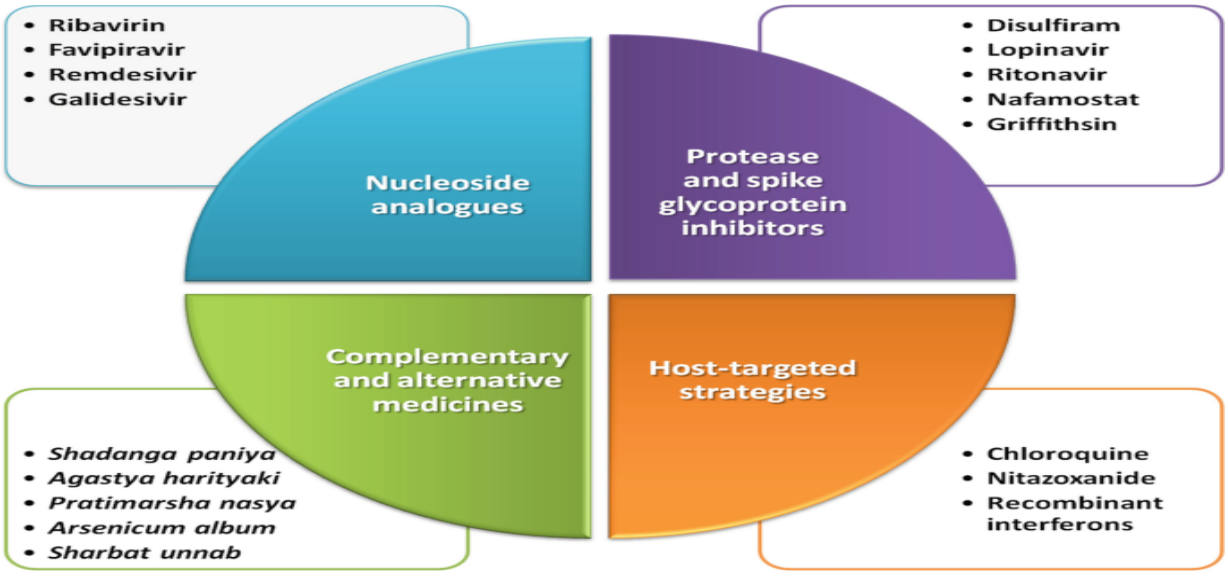

Figure 1: Investigational treatment approaches of COVID-19

Although there were asymptomatic patients that relied on the efficacy of immune-induced suppression of the viral-loads, patients that shown severe symptoms such as sepsis and rapid respiratory failure were closely monitored. In case of severe respiration arrest or shock, hypxemia and distress behaviours, ventilators were used and other supplementary oxygen therapy to provide immediate supportive treatment. In one hand, Alternative Medicine which encompasses homeopathy, naturopathy, and tradomedical products that were used MERS-COVs and SARS-COVs demonstrated efficacy against coronaviruses with minimal reports on adverse effects. On the other hand, some vaccines were approved by WHO including Pfizer/BioNTech(first vaccine approved), others including Moderna, Janssen J & J, SII/COVIDSHIELD, AstraZeneca/AZD122, Sinopharm, Sinovac-CoronaVac,

Bharat Biotech BBV152 COVAXIN, Nuvaxovid [27]. In Akwa Ibom state, 63,336, and 69,030 doses of Moderna and AstraZeneca vaccines were received respectively. The Akwa Ibom State Ministry of Health in an emergency covid-19 report on August, 2021 has it that, about 14% and 95% of the two brands of vaccines were administered respectively. These interventions were very strategic in managing and controlling the spread of the infectious disease, but it becomes a necessity to assess the effectiveness of these measure in preparation for subsequence occurrence.

Consequently, mathematical and computational modelling remain instrumental to addressing such challenges after the declaration of an end to COVID-19 by WHO. Mathematical modelling has been used to investigate the dynamical behaviour and control measures of COVID-19[27] in the presence of delta and omicron with vaccination and non-pharmaceutical interventions. They unfolded that omicron variant is more transmissible than other variants. They recommended a continued combination of non-pharmaceutical interventions with vaccination programs to control the disease outbreak. The impact of vaccination strategies on the spread of COVID-19 has been investigated in [14], via mathematical modelling approach. Based on the results from sensitivity analysis, they opined that vaccination rate, contact tracing, rapid testing are the most important parameters that reduced the effective reproduction number of the virus. Analogously, the impact of testing and isolation compliance on the transmission of COVID-19 in its early stage was investigated in [7]. Using the qualitative properties of the model, they highlighted that the daily infection peak showed high testing rates and high isolation compliance reduced the prevalence of the infection remarkably. In the same vein, a classical Susceptible, Exposed, Infected and Recovery (SEIR)-Model [31] has been modified to incorporate compartments for vaccinated, asymptomatic, hospitalized, and deceased individuals. Through the alteration of the modelling parameters, it was revealed that vaccination rate, immunity loss, and relaxation of measures regarding the vaccinated individuals affect the dynamics of COVID-19 spread. There was an exponential increase in the death rate during the dominance of the delta variant and before the initiation of the booster shot program. Also, the co-dynamical properties of COVID-19 and tuberculosis has been investigated in [20] , and a deterministic inversion reproduction of the two infectious diseases were obtained. Using numerical simulation of the fitted datasets, they reported that COVID-19 incidence decreases with co-infection prevalence, then the burden of tuberculosis on the human population increases. Using the optimal control theory in [15] , a combination of the effect of COVID-19 vaccination and exogenous reinfection for tuberculosis(TB). In the analytic result, reducing the basic reproduction ($R_0 < 1$) was not sufficient to eliminate the disease from the community, because of co-morbidity of COVID-19, with tuberculosis (TB). Inspite the foregoing models, this paper proposes a much more realistic and deterministic model of the spread or transmission and control of the infectious disease, with logistic function as per capita influx varying functional to control the susceptibility and infectivity of the system.

1.1 Description and Formulation of Mathematical Model of COVID-19

Considering the total population of individuals at time t, $N(t)$, and it deterministic subpopulations as (a) Total susceptible individuals to COVID-19 at time t, $S(t)$. This includes the total infectible class of individuals subject to the environmental carrying capacity of the entire population (b) Total exposed individuals to COVID-19 at time t, $E(t)$. This entails numerous frontline health-works, and people at high risk to contracting the infection, after due contact with the infected person with and without any visible symptoms during contact tracing. (c) Total asymptomatic infected class of individuals with COVID-19 at time t, $A(t)$. This connotes individuals that are infectious to others without any visible symptoms of the infection after contact tracing programme. They are suggested to have high immune efficacy to suppress and delay the viral loads of the infection, and can recovered from the infection without treatment. The asymptomatic class of individuals, may have exceeded the initial incubation period (i.e., seven to fourteen days) of the infection (d) Total infected and infectious individuals with COVID-19 at time t, $I(t)$. This population registered the incident case of COVID-19 in the entire population. In this model, the total active cases of the population with

COVID-19 is derived from NCDC, during the epic-week of the infection in Akwa Ibom State, see figure 2 below (e) Total hospitalized individual with COVID-19 at time t, $H(t)$. This population is quarantined, and get treated of the infection after being diagnosed of symptoms of COVID-19. They were quarantine or self-isolated for treatment and (f) Total individuals that recovered from COVID-19, after treatment or through immune efficacy, at time t, $R(t)$. For biological relevance, all subpopulations are subject to positive initial population, and the entire population, is represented in a functional space region given as follows:

$$\begin{cases} N(t) = & S(t)+E(t)+A(t)+I(t)+H(t)+R(t) | (S(t),E(t),A(t),I(t),H(t),R(t)) > 0 \\ & S(t)=S_0, E(t)=E_0, A(t)=A_0, I(t)=I_0, H(t)=H_0, R(t)=R_0, \forall\ t \geq 0 \\ & S_0>0, E_0>0, A_0>0, I_0>0, H_0>0, R_0>0 \\ \Omega = & (S(t),E(t),A(t),I(t),H(t),R(t)) \in \mathbb{R}^6_+ | 0 \leq N(t) \leq N_{max} \end{cases} \tag{1.1}$$

Equation 1.1 defines a positive invariant region, well possedness, and boundedness of the model for epidemiological relevance. It forms a solution space as Ω-attractor sets of plausible dynamics of COVID-19 pandemic. Hence solution that are in the Ω remains in $\Omega\ \forall\ t \geq 0$. Using the state variables of the model, the targeted population $N(t)$ can be recruited to the susceptible class of individuals via a logistic growth function $\alpha S(t)\left(1-\frac{S(t)}{\kappa}\right)$. There is a restriction in the population of the susceptible class based on rumours of spontaneous spread of the infection, and enforcement of total lockdown using the parameter, κ. The parameter, α measures the recruitment rate from the targeted population to the susceptible class of individuals, due to natural birth rate or immigration. The transmission rate from susceptible class to symptomatically infected class, and exposed class, are denoted by β and μ respectively. Almost all exposed individuals are transfered to the infected class and asymptomatic class by the fractions $\epsilon(\rho-1), \rho \neq 1$, and $\epsilon\rho$ respectively, where ϵ is the transmission rate. The paramer ρ depicts an adjustment for uncertainty in proportional movement, after contact tracing. The rate in which the infected class of individuals are transfered to the hospitalized class, is denoted by ψ, with recovery rate, η. Aslo, the asymptomatic individuals, recovers at the rate δ, and transfered to the recovery class. Each subpopulation, namely susceptible, exposed, asymptomatic, infected, hospitalized, and recovery classes, decreases by the natural death rate, denoted by σ, respectively. The COVID-19 induced death rate for exposed, asymptomatic, infected, and hospitalized individuals are denoted by ϱ, ζ, ν and ω respectively. The assumptions of the model include the following:

- The targeted population is non-homogeneous, as there is restriction on the carrying capacity, where the susceptible class can be infected or exposed to the pandemic. This implies that some individuals had already practiced self-isolation, before the epi-week of the infection in the state.
- The model incooperates uncertain parameter (ξ) on the fatality rate of the infection as some persons that died naturally were attributed to co-morbidity in COVID-19 after recovery from the infection. Thus, individuals in each group has equal natural death rate, excluding the recovery class of individuals.
- Non-proportionate movement of exposed class of individuals to infected and asymptomatic class of individuals, respectively. Since natural immunity can reduce the viral-load, and the individual can recover from the disease.
- The model datasets are estimated using the NCDC bi-weekly epidemiological report of COVID-19 peculiar to Akwa Ibom State, between 1st to 30th August, 2021.
- Zonootic infectiousness of the viral disease has been neglected.

The proposed mathematical model that depicts the nonlinear dynamics; transmission and transfer within the subpopulations leads to the following system of ordinary differential equation 1.2. The

model in equation 1.2 is subject to the initial condition in equation 1.1.

$$\begin{cases} \frac{dS}{dt} = & \alpha S(t)\left(1-\frac{S(t)}{K}\right) - \beta S(t)E(t) - \mu S(t)I(t) - \sigma S(t) \\ \frac{dE}{dt} = & \beta S(t)E(t) - \epsilon(\rho-1)E(t) - (\varrho+\sigma)E(t) \\ \frac{dI}{dt} = & \mu S(t)I(t) + \epsilon\rho E(t) - \psi I(t) - (\zeta+\sigma)I(t) \\ \frac{dA}{dt} = & \epsilon(\rho-1)E(t)) - \delta A(t) - (\nu+\sigma)A(t) \\ \frac{H}{dt} = & \psi I(t) - \eta H(t) - (\omega+\sigma)H(t) \\ \frac{dR}{dt} = & \delta A(t) + \eta H(t) - (\xi+\sigma)R(t) \end{cases} \tag{1.2}$$

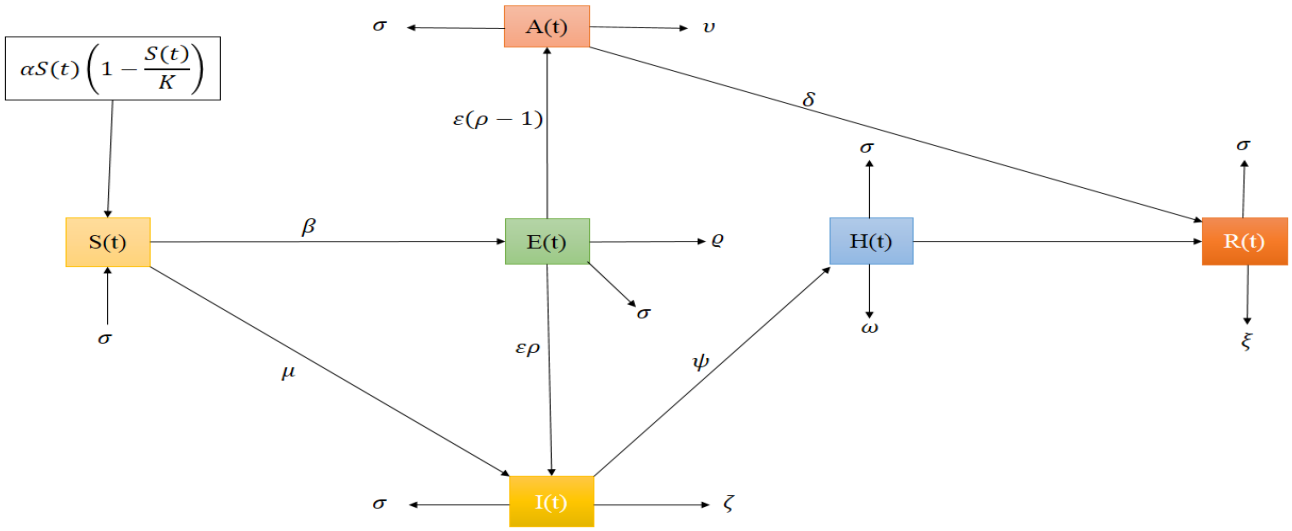

Figure 2: structural modelling of the subpopulations and epidemiological parameters of COVID-19

Epidemiological interactions of the state variables and parameters is given in figure 2. The following theorem is used to establish the boundedness of the epidemiological parameters within positive invariant region.

1.2 Functional Analytic and Uniform Convergence in COVID-19 Model

Theorem 1 [10]**:** Define a time-dependent vector space of the model in equations 1.1 and 1.2 as $\boldsymbol{X} = (S(t), E(t), A(t), I(t), H(t), R(t))^T$ on a continuously differentiable functional $\boldsymbol{F} \in C^1$ such that $\boldsymbol{F} : \boldsymbol{J} \times \boldsymbol{R}^6_+ \to \boldsymbol{R}^6_+$ is relatively compact in $\boldsymbol{F}(\boldsymbol{\Omega})$ with a smooth dynamic phase flow $\phi_t(t_0, \boldsymbol{X})$. Given that $\boldsymbol{\Omega}$ is a closed, convex, and non-empty subset of a Banach space in $\boldsymbol{R}^6_+$, then the couple set of first order differential equation

$$\begin{cases} \dot{\boldsymbol{X}}(t) = \boldsymbol{F}(\boldsymbol{X})(t); \;\; t \in [0,T] = \boldsymbol{J} \\ \boldsymbol{X}(0) = \boldsymbol{X_0} = (S_0, E_0, A_0, I_0, H_0, R_0) \in \boldsymbol{R}^6_+ \end{cases} \tag{1.3}$$

has a unique solution.

Remark: Since $\boldsymbol{F} \in C^1$, the $\boldsymbol{F}$ is locally Lipschitz. Theorem 1 guarantees the existence and uniqueness of solution of equations 1.1 and 1.2 with sensitive dependence on initial conditions. The following lemma guides the prove of this theorem.

Lemma 1:[5] If $p, q \geq 1$ is define with conjugacy $\frac{1}{p} + \frac{1}{q} = 1$, then $\frac{1}{p}x^p + \frac{1}{q}y^q \geq xy \;\; \forall\, x, y \geq 0$.

Lemma 2: Gronwalls' Inequality [10]: Let $u : [0,T] \longrightarrow \boldsymbol{R}$ be continuous and non-negative. Suppose $C \geq 0$ and $K \geq 0$ are such that

$$U(t) \leq C + \int_{t_0}^{t} KU(s)ds \tag{1.4}$$

for all $(t, t_0) \in [0,T]$. Then, for all t in this interval,

$$U(t) \leq Ce^{K(t-t_0)} \tag{1.5}$$

Lemma 3: Suppose $U_k : J \to \boldsymbol{R}^n,\ k = 0, 1, 2, ...,$ is a sequence of continuous functions on a closed interval J such that given $\epsilon > 0$ there is some $N > 0$, and for every $p, q > N$ such that

$$max_{t\in J}|U_p(t) - U_q(t)| < \epsilon \tag{1.6}$$

Then there is a continuous function $U : J \to \boldsymbol{R}^n$ such that

$$max_{t\in J}|U_k(t) - U(t)| \to 0 \ \text{ as } \ k \to \infty \tag{1.7}$$

Moreover, for any t with $|t| \leq h,\ \ U_0(0) < M$

$$\lim_{t\to\infty} \int_0^t U_k(s)ds = \int_0^t U(s)ds \tag{1.8}$$

Remark: This lemma establishes the uniform convergence of any sequence of continuous function using Picard's iteration scheme.

Proof: It suffices to show that the vector-valued functional $\boldsymbol{F}$ is a contractive map. Define two analytic and integral solutions of the considered system in eqn1.1 and 1.2 as nonlinear continuous functionals $\boldsymbol{X}, \boldsymbol{Y} : \boldsymbol{J} \times \boldsymbol{R}_+^{\boldsymbol{6}} \to \boldsymbol{R}$. In closed form, these functions are equivalent solutions to the model defined in equations 1.1 and 1.2 can be written as:

$$\begin{aligned} \boldsymbol{X}(t) =& \boldsymbol{X_0} + \int_{t_0}^{t} \boldsymbol{F}(\boldsymbol{X})(\boldsymbol{s})ds \\ \boldsymbol{Y}(t) =& \boldsymbol{Y_0} + \int_{t_0}^{t} \boldsymbol{F}(\boldsymbol{Y})(\boldsymbol{s})ds \end{aligned} \tag{1.9}$$

Geometrically, assume that for all initial solutions that are closed together, any solution that passes through them remain close at all time, then given $\epsilon^* > 0$ there exist δ^* such that $\|X_0 - Y_0\| < \delta^*$ and

$$|\boldsymbol{X}(\boldsymbol{s}) - \boldsymbol{Y}(\boldsymbol{s})| \leq |\boldsymbol{X_0} - \boldsymbol{Y_0}| + \int_{t_0}^{t} |(\boldsymbol{F}(\boldsymbol{s}), \boldsymbol{X}(\boldsymbol{s})) - \boldsymbol{F}(\boldsymbol{s}, \boldsymbol{Y}(\boldsymbol{s}))|ds \tag{2.0}$$

Apply triangle inequality, and lemma 2 then equation 2.0 yields

$$\begin{cases} \|\boldsymbol{X}(\boldsymbol{s}) - \boldsymbol{Y}(\boldsymbol{s})\| \leq \|\boldsymbol{X_0} - \boldsymbol{Y_0}\| e^{\|\boldsymbol{K}\|h} < \epsilon^*; \ \ h \in [0,T], \\ \qquad\qquad\qquad \leq \delta^* e^{\|\boldsymbol{K}\|h} < \epsilon^*; \ \ h \in [0,T], \\ \|\boldsymbol{K}\| = \max\limits_{1\leq j\leq 6} \sum\limits_{i=1}^{6} |A_{i,j}|, \ \ \rho^*(A_{i,j}) \leq \|A_{i,j}\| \end{cases} \tag{2.1}$$

where ρ^* is the spectral radius of the matrix, $A_{i,j}$. The square matrix $A_{i,j}$, equiped with the norm $\max\limits_{0\leq i\leq 6} (\|\boldsymbol{X_i}\|, \|\boldsymbol{Y_i}\|) \leq \phi$ is define as follows,

$$\begin{bmatrix} (\alpha + \frac{2\alpha\phi}{K} + \phi(\beta + \mu) + \sigma) & \beta\phi & \mu\phi & 0 & 0 & 0 \\ \beta\phi & \beta\phi + \epsilon(\rho - 1) + (\varrho + \sigma) & 0 & 0 & 0 & 0 \\ \mu\phi & \epsilon\rho & \mu\phi + \psi + \zeta + \sigma & 0 & 0 & 0 \\ 0 & (\epsilon\rho - 1) & 0 & \delta + \nu + \sigma & 0 & 0 \\ 0 & 0 & \psi & 0 & \eta + \omega + \sigma & 0 \\ 0 & 0 & 0 & 0 & 0 & \xi + \sigma \end{bmatrix}$$

By choosing $\delta^* = \frac{\epsilon^*}{e^{\|K\|h}}$, the operator $\boldsymbol{F}$ on $\boldsymbol{X}, \boldsymbol{Y}$ is a contractive map. Using Lemma 3 for identical initial conditions, say $\|\boldsymbol{X_0} - \boldsymbol{Y_0}\| = 0$, then $\boldsymbol{X(s)} = \boldsymbol{Y(s)}$. Hence the prove is complete.

Corollary: *Model of system 1.1 and 1.2 is ultimately bounded in the positive invariant region of* $\boldsymbol{\Omega} \subset \mathbb{R}^6_+$ *if* $\frac{\epsilon^*}{exp(\|K\|h)} < 1$.

Remark: This theorem establishes the analytic solution profile of equations 1.1 and 1.2, using the fundamental theory of functional analysis. Since a uniformly continuous functions is ultimately bounded.

2.0 Dynamics at Equilibrium Points in COVID-19 Model

2.1 Existence of Positive Equilibrium Points in the Model:

The steady state behaviour of the model defines the disease free equilibrium(E_0), and endemic equilibrium (E_1) points of the model given as

$$
\begin{cases}
E_0^* & = \left(S_0^* = \frac{\kappa\,(\alpha-\sigma)}{\alpha}, E_0^* = 0, I_0^* = 0, A_0^* = 0, H_0^* = 0, R_0^* = 0\right)\ E_1^* = \left(S_1^*, E_1^*, I_1^*, A_1^*, H_1^*, R_1^* = \frac{P^*}{Q^*}\right) \\
S_1^* & = \left(\frac{\rho\epsilon+\sigma+\varrho-\epsilon}{\beta}\right),\ E_1^* = \frac{(-\mu\,\rho\,\varepsilon+\beta\,\psi+\beta\,\sigma+\beta\,\varsigma-\mu\,\sigma-\mu\,\varrho+\mu\,\varepsilon)(\alpha\,\beta\,\kappa-\alpha\,\rho\,\varepsilon-\beta\,\kappa\,\sigma-\alpha\,\sigma-\alpha\,\varrho+\alpha\,\varepsilon)}{\beta^2\kappa\,(\beta\,\psi+\beta\,\sigma+\beta\,\varsigma-\mu\,\sigma-\mu\,\varrho+\mu\,\varepsilon)} \\
A_1^* & = \frac{\varepsilon\,(\alpha\,\beta\,\kappa-\alpha\,\rho\,\varepsilon-\beta\,\kappa\,\sigma-\alpha\,\sigma-\alpha\,\varrho+\alpha\,\varepsilon)\left(-\mu\,\rho^2\varepsilon+\beta\,\psi\,\rho+\beta\,\rho\,\sigma+\beta\,\rho\,\varsigma-\mu\,\rho\,\sigma-\mu\,\rho\,\varrho+2\,\mu\,\rho\,\varepsilon-\beta\,\psi-\beta\,\sigma-\beta\,\varsigma+\mu\,\sigma+\mu\,\varrho-\mu\,\varepsilon\right)}{\beta^2\kappa(\sigma+\delta+\upsilon)(\beta\,\psi+\beta\,\sigma+\beta\,\varsigma-\mu\,\sigma-\mu\,\varrho+\mu\,\varepsilon)}, \\
I_1^* & = \frac{(\alpha\,\beta\,\kappa-\alpha\,\rho\,\varepsilon-\beta\,\kappa\,\sigma-\alpha\,\sigma-\alpha\,\varrho+\alpha\,\varepsilon)\varepsilon\,\rho}{(\beta\,\psi+\beta\,\sigma+\beta\,\varsigma-\mu\,\sigma-\mu\,\varrho+\mu\,\varepsilon)\beta\,\kappa} \\
H_1^* & = \frac{\psi\,\rho\,\varepsilon\,(\alpha\,\beta\,\kappa-\alpha\,\rho\,\varepsilon-\beta\,\kappa\,\sigma-\alpha\,\sigma-\alpha\,\varrho+\alpha\,\varepsilon)}{\beta\,\kappa\,(\beta\,\eta\,\psi+\beta\,\eta\,\sigma+\beta\,\eta\,\varsigma+\beta\,\omega\,\psi+\beta\,\omega\,\sigma+\beta\,\omega\,\varsigma+\beta\,\psi\,\sigma+\beta\,\sigma^2+\beta\,\sigma\,\varsigma-\eta\,\mu\,\sigma-\eta\,\mu\,\varrho+\eta\,\mu\,\varepsilon-\mu\,\omega\,\sigma-\mu\,\omega\,\varrho+\mu\,\omega\,\varepsilon-\mu\,\sigma^2-\mu\,\sigma\,\varrho+\mu\,\sigma\,\varepsilon)} \\
P^* & = \varepsilon(-\delta\,\eta\,\mu\,\rho^2\varepsilon - \delta\,\mu\,\omega\,\rho^2\varepsilon - \delta\,\mu\,\rho^2\sigma\,\varepsilon + 2\,\beta\,\delta\,\eta\,\psi\,\rho + \beta\,\delta\,\eta\,\rho\,\sigma + \beta\,\delta\,\eta\,\rho\,\varsigma + \beta\,\delta\,\omega\,\psi\,\rho + \\
& \quad \beta\,\delta\,\omega\,\rho\,\sigma + \beta\,\delta\,\omega\,\rho\,\varsigma + \beta\,\delta\,\psi\,\rho\,\sigma + \beta\,\delta\,\rho\,\sigma^2 + \beta\,\delta\,\rho\,\sigma\,\varsigma + \beta\,\eta\,\psi\,\rho\,\sigma + \beta\,\eta\,\psi\,\rho\,\upsilon - \delta\,\eta\,\mu\,\rho\,\sigma - \\
& \quad \delta\,\eta\,\mu\,\rho\,\varrho + 2\,\delta\,\eta\,\mu\,\rho\,\varepsilon - \delta\,\mu\,\omega\,\rho\,\sigma - \delta\,\mu\,\omega\,\rho\,\varrho + 2\,\delta\,\mu\,\omega\,\rho\,\varepsilon - \delta\,\mu\,\rho\,\sigma^2 - \delta\,\mu\,\rho\,\sigma\,\varrho + 2\,\delta\,\mu\,\rho\,\sigma\,\varepsilon - \\
& \quad \beta\,\delta\,\eta\,\psi - \beta\,\delta\,\eta\,\sigma - \beta\,\delta\,\eta\,\varsigma - \beta\,\delta\,\omega\,\psi - \beta\,\delta\,\omega\,\sigma - \beta\,\delta\,\omega\,\varsigma - \beta\,\delta\,\psi\,\sigma - \beta\,\delta\,\sigma^2 - \beta\,\delta\,\sigma\,\varsigma + \\
& \quad \delta\,\eta\,\mu\,\sigma + \delta\,\eta\,\mu\,\varrho - \delta\,\eta\,\mu\,\varepsilon + \delta\,\mu\,\omega\,\sigma + \delta\,\mu\,\omega\,\varrho - \delta\,\mu\,\omega\,\varepsilon + \delta\,\mu\,\sigma^2 + \delta\,\mu\,\sigma\,\varrho - \delta\,\mu\,\sigma\,\varepsilon) \\
& \quad (\alpha\,\beta\,\kappa - \alpha\,\rho\,\varepsilon - \beta\,\kappa\,\sigma - \alpha\,\sigma - \alpha\,\varrho + \alpha\,\varepsilon) \\
Q^* & = \beta^2\kappa(\beta\,\eta\,\psi + \beta\,\eta\,\sigma + \beta\,\eta\,\varsigma + \beta\,\omega\,\psi + \beta\,\omega\,\sigma + \beta\,\omega\,\varsigma + \beta\,\psi\,\sigma + \beta\,\sigma^2 + \beta\,\sigma\,\varsigma - \eta\,\mu\,\sigma - \eta\,\mu\,\varrho + \\
& \quad \eta\,\mu\,\varepsilon - \mu\,\omega\,\sigma - \mu\,\omega\,\varrho + \mu\,\omega\,\varepsilon - \mu\,\sigma^2 - \mu\,\sigma\,\varrho + \mu\,\sigma\,\varepsilon)
\end{cases}
\tag{eqn 2.2}
$$

2.2 Basic Reproduction Number(R_0) of COVID-19:

The basic reproduction number (R_0) is a dimensionless parameter that determines an average spread of the disease by a infectious person during contact with the susceptible, exposed, asymptomatic and hospitalized populations. The expected spreading parameter quantifies continuous spread for infection if $R_0 > 1$, and extinction of the spread if $R_0 < 1$ near the disease free equilibrium point in the model. In this model the sub-populations that are responsible for spreading the disease are exposed, $E(t)$; infected $E(t)$; asymptomatic, $A(t)$; and hospitalized, $H(t)$ classes. Using the Next Generation Operator[17] at the disease free equilibrium (E_0) in system of eqn 2.2 , a compartmental subsystem of transmission and transfer matrices (F, V) are obtained as follow. In this case, the

basic reproduction number (R_0) is the spectral radius of the matrix operator; FV^{-1}

$$\begin{cases} F = & \begin{bmatrix} \frac{\beta\kappa\,(\alpha-\sigma)}{\alpha} & 0 & 0 & 0 \\ 0 & \frac{\mu\,\kappa\,(\alpha-\sigma)}{\alpha} & 0 & 0 \\ 0 & 0 & 0 & 0 \\ 0 & 0 & 0 & 0 \end{bmatrix} \\ V = & \begin{bmatrix} \varrho+\sigma+\varepsilon\ (\rho-1) & 0 & 0 & 0 \\ -\varepsilon\,\rho & \psi+\sigma+\varsigma & 0 & 0 \\ -\varepsilon\ (\rho-1) & 0 & \delta+\upsilon+\sigma & 0 \\ 0 & -\psi & 0 & \eta+\omega+\sigma \end{bmatrix} \\ V^{-1} = & \begin{bmatrix} (\varepsilon\,\rho+\sigma+\varrho-\varepsilon)^{-1} & 0 & 0 & 0 \\ \frac{\varepsilon\,\rho}{(\varepsilon\,\rho+\sigma+\varrho-\varepsilon)(\psi+\sigma+\varsigma)} & (\psi+\sigma+\varsigma)^{-1} & 0 & 0 \\ \frac{\varepsilon\,(\rho-1)}{(\varepsilon\,\rho+\sigma+\varrho-\varepsilon)(\delta+\upsilon+\sigma)} & 0 & (\delta+\upsilon+\sigma)^{-1} & 0 \\ \frac{\psi\,\varepsilon\,\rho}{(\varepsilon\,\rho+\sigma+\varrho-\varepsilon)(\psi+\sigma+\varsigma)(\eta+\omega+\sigma)} & \frac{\psi}{(\psi+\sigma+\varsigma)(\eta+\omega+\sigma)} & 0 & (\eta+\omega+\sigma)^{-1} \end{bmatrix} \\ P(FV^{-1},\lambda) = & \lambda^4 - \frac{\kappa\,(\alpha-\sigma)(\mu\,\rho\,\varepsilon+\beta\,\psi+\beta\,\sigma+\beta\,\varsigma+\mu\,\sigma+\mu\,\varrho-\mu\,\varepsilon)\lambda^3}{\alpha\,(\varepsilon\,\rho+\sigma+\varrho-\varepsilon)(\psi+\sigma+\varsigma)} + \frac{\mu\,\kappa^2(\alpha-\sigma)^2\beta\,\lambda^2}{\alpha^2(\psi+\sigma+\varsigma)(\varepsilon\,\rho+\sigma+\varrho-\varepsilon)},\ \lambda_1 = \frac{\mu\,\kappa\,(\alpha-\sigma)}{\alpha\,(\psi+\sigma+\varsigma)}, \\ & \lambda_2 = \frac{\beta\,\kappa\,(\alpha-\sigma)}{\alpha\,(\varepsilon\,\rho+\sigma+\varrho-\varepsilon)} \\ R_0 = \rho(FV^{-1}) = & \max(\lambda_1,\lambda_2) = \frac{\beta\,\kappa\,(\alpha-\sigma)}{\alpha\,(\varepsilon\,\rho+\sigma+\varrho-\varepsilon)} \end{cases} \tag{eqn 2.3}$$

Lemma 4[1] Let $A \in \mathbb{R}^{n\times n}$ be a real matrix, with $P(\lambda) = \det|\lambda I - A| = a_0\lambda^n + a_1\lambda^{n-1} + \cdots + a_{n-1}\lambda + a_n = 0$. If $a_i > 0 (i = 1, 2, \ldots, n)$, then $P(\lambda)$ is Hurwitzian if and only if

$$\begin{cases} \Delta_1 = a_1 > 0,\ \Delta_2 = \begin{vmatrix} a_1 & a_0 \\ a_3 & a_2 \end{vmatrix} > 0, \Delta_3 = \begin{vmatrix} a_1 & a_0 & 0 \\ a_3 & a_2 & a_1 \\ a_5 & a_4 & a_3 \end{vmatrix} > 0, \\ \Delta_n = \begin{vmatrix} a_1 & a_0 & 0 & 0 & 0 & \cdots & 0 & 0 & 0 & 0 \\ a_3 & a_2 & a_1 & 0 & 0 & 0 & \cdots & 0 & 0 & 0 \\ a_5 & a_4 & a_3 & a_2 & a_1 & 0 & 0 & \cdots & 0 & 0 \\ \cdots & \cdots & & & & & & & \cdots & \cdots \\ \cdots & \cdots & & & & & & & a_{n-1} & a_{n-2} \\ a_{2n-1} & a_{2n-2} & \cdots & \cdots & \cdots & \cdots & \cdots & \cdots & \cdots & a_n \end{vmatrix} = \Delta_{n-1}a_n > 0, \end{cases} \tag{eqn 2.4}$$

where $a_s = 0\ \forall\ s < 0$ or $s > n$.

Lemma 5 (Descarte's Rule of Sign)[1]: Consider the sequence of coefficient of real polynomial $P_n(\lambda) = a_n\lambda^n + a_{n-1}\lambda^{n-1} + \cdots + a_1\lambda + a_0$ defined as $\{a_n\}_{i=0}^{i=n}$. Let k be the total number of sign changes from one coefficient to the next in the sequence, then the number of positive roots of the polynomial is either equal to k or $k - 2m$, where m is an even integer. (Note, if $k = 1$, then there is exactly one positive real root).

Theorem 2: The disease free equilibrium point E_0 of equation 1.2 is locally asymptotically stable if $R_0 < 1$, and unstable if $R_0 > 1$.

Proof

The Jacobian matrix of the model 1.2 and 1.2, evaluated that the disease free equilibrium is given

in equation 2.5, as well as the characteristic polynomial and corresponding eigenvalues.

$$
\begin{cases}
J_{ij}(E_0) = \begin{bmatrix}
-\alpha+\sigma & -\frac{\beta\,\kappa\,(\alpha-\sigma)}{\alpha} & -\frac{\mu\,\kappa\,(\alpha-\sigma)}{\alpha} & 0 & 0 & 0 \\
0 & J_{22} & 0 & 0 & 0 & 0 \\
0 & \varepsilon\,\rho & \frac{\mu\,\kappa\,(\alpha-\sigma)}{\alpha}-\psi-\sigma-\varsigma & 0 & 0 & 0 \\
0 & \varepsilon\,(\rho-1) & 0 & -\delta-\sigma-\upsilon & 0 & 0 \\
0 & 0 & \psi & 0 & -\eta-\omega-\sigma & 0 \\
0 & 0 & 0 & \delta & \eta & -\xi-\sigma
\end{bmatrix} \\
\textit{where} \\
J_{22} = \frac{\alpha(-\varrho-\sigma-\varepsilon\,(\rho-1)+\beta\,\kappa\,)(\alpha-\sigma)}{\alpha} \\
P(\lambda) = \lambda^6-(J_{11}J_{22}J_{33}J_{44}J_{55}J_{66})\lambda^5+(J_{11}J_{22}+J_{11}J_{33}+J_{11}J_{44}+J_{11}J_{55}+J_{11}J_{66}+J_{33}J_{22} \\
+J_{44}J_{22}+J_{55}J_{22}+J_{66}J_{22}+J_{33}J_{44}+J_{33}J_{55}+J_{33}J_{66}+J_{55}J_{44}+J_{66}J_{44}+J_{55}J_{66} \\
-J_{56}J_{65})\lambda^4+(-J_{11}J_{22}J_{33}-J_{11}J_{22}J_{44}-J_{11}J_{22}J_{55}-J_{11}J_{22}J_{55}-J_{11}J_{33}J_{44}-J_{11}J_{33}J_{55} \\
-J_{11}J_{33}J_{66}-J_{11}J_{44}J_{55}-J_{11}J_{44}J_{66}-J_{11}J_{55}J_{66}+J_{11}J_{56}J_{65}-J_{22}J_{33}J_{44}-J_{22}J_{33}J_{55} \\
J_{22}J_{33}J_{66}-J_{22}J_{55}J_{44}-J_{22}J_{66}J_{44}-J_{22}J_{55}J_{66}+J_{22}J_{56}J_{65}-J_{33}J_{44}J_{55}-J_{33}J_{44}J_{66} \\
-J_{33}J_{55}J_{66}+J_{33}J_{56}J_{65}-J_{44}J_{55}J_{66}+J_{44}J_{56}J_{65})\lambda^3+(J_{11}J_{22}J_{33}J_{44}+J_{11}J_{22}J_{33}J_{55} \\
J_{11}J_{22}J_{33}J_{66}+J_{11}J_{22}J_{44}J_{55}+J_{11}J_{22}J_{44}J_{66}+J_{11}J_{22}J_{55}J_{66}-J_{11}J_{22}J_{56}J_{65} \\
+J_{11}J_{33}J_{44}J_{55}-J_{11}J_{66}J_{33}J_{44}-J_{11}J_{44}J_{56}J_{65}+J_{22}J_{33}J_{44}J_{55}+J_{22}J_{33}J_{44}J_{66} \\
-J_{22}J_{33}J_{56}J_{65}+J_{22}J_{44}J_{55}J_{66}-J_{22}J_{44}J_{56}J_{65}+J_{33}J_{44}J_{55}J_{66}-J_{33}J_{44}J_{56}J_{65})\lambda^2+ \\
(-J_{11}J_{22}J_{33}J_{44}J_{55}-J_{11}J_{22}J_{33}J_{44}J_{66}-J_{11}J_{22}J_{33}J_{66}J_{55}+J_{11}J_{22}J_{33}J_{56}J_{65} \\
-J_{11}J_{22}J_{44}J_{66}J_{55}+J_{11}J_{22}J_{44}J_{56}J_{65}-J_{11}J_{33}J_{44}J_{55}J_{66}+J_{22}J_{33}J_{44}J_{56}J_{65})\lambda \\
+J_{11}J_{22}J_{33}J_{44}J_{55}J_{66}-J_{11}J_{22}J_{33}J_{44}J_{56}J_{65} \\
\textit{and} \\
\lambda_1=-\xi-\sigma\,,\lambda_2=-\alpha+\sigma\,,\lambda_3=\frac{\alpha\,\kappa\,\mu-\mu\,\kappa\,\sigma-\alpha\,\psi-\alpha\,\sigma-\alpha\,\varsigma}{\alpha}\,,\lambda_4=-\eta-\omega-\sigma\,, \\
\lambda_5=-\delta-\sigma-\upsilon\,,\lambda_6=\frac{\alpha\,\beta\,\kappa-\alpha\,\rho\,\varepsilon-\beta\,\kappa\,\sigma-\alpha\,\sigma-\alpha\,\varrho+\alpha\,\varepsilon}{\alpha}
\end{cases}
\tag{2.5}
$$

Then, ensuring that all eigenvalues identified in 2.5 are negatives; $(\alpha>\sigma,\lambda_{i\ (i=1,2,...6)}<0)$ guarantees $R_0=\frac{\beta\,\kappa\,(\alpha-\sigma)}{\alpha\,(\varepsilon\,\rho+\sigma+\varrho-\varepsilon)}<1$ or otherwise and the prove is complete.

Theorem 3: The endemic equilibrium point (E_1) defined in eqn 2.2 is locally asymptotically stable for $R_0>1$

Proof Assume that the basic reproduction number $R_0>1$, then the endemic equilibrium point exist. Evaluating the Jacobian matrix of 1.2 at the endemic equilibrium (E_1) point yields:

$$
\begin{cases}
J_{ij}(E_1) = \begin{bmatrix}
-\frac{\alpha\,(\varepsilon(\rho-1)+\sigma+\varrho)}{\beta\kappa} & -\rho\varepsilon-\sigma-\varrho+\varepsilon & -\frac{(\varepsilon(\rho-1)+\sigma+\varrho)\mu}{\beta} & 0 & 0 & 0 \\
J_{21} & 0 & 0 & 0 & 0 & 0 \\
J_{31} & \rho\varepsilon & J_{33} & 0 & 0 & 0 \\
0 & \varepsilon\,(\rho-1) & 0 & -\delta-\sigma-\upsilon & 0 & 0 \\
0 & 0 & \psi & 0 & -\eta-\omega-\sigma & 0 \\
0 & 0 & 0 & \delta & \eta & -\xi-\sigma
\end{bmatrix} \\
J_{21}=\frac{(-\beta\kappa(\alpha-\sigma)+\alpha(\varepsilon(\rho-1)+\sigma+\varrho))((-\psi-\sigma-\varsigma)\beta+(\varepsilon(\rho-1)+\sigma+\varrho)\mu)}{\beta\kappa((\psi+\sigma+\varsigma)\beta+\mu(-\sigma-\varrho+\varepsilon))}, \\
J_{31}=-\frac{(-\beta\kappa(\alpha-\sigma)+\alpha(\varepsilon(\rho-1)+\sigma+\varrho))\rho\,\varepsilon\mu}{\beta\kappa((\psi+\sigma+\varsigma)\beta+\mu(-\sigma-\varrho+\varepsilon))}, \\
J_{33}=\frac{(-\psi-\sigma-\varsigma)\beta+(\varepsilon(\rho-1)+\sigma+\varrho)\mu}{\beta},\ \forall\,i,j\ 1,2,...,6
\end{cases}
\tag{2.6}
$$

Using the entries of the Jacobian matrix in system 2.6, to construct the corresponding characteristic polynomial 2.7 at the endemic equilibrium point, and applying lemma 4 yields the required result as follow. Recall that lemma 4 guarantees the existence of negative roots of the given polynomial in eqn 2.7

$$\begin{cases} P(\lambda) = & \lambda^6 + (-J_{66} - J_{55} - J_{44} - J_{33} - J_{11})\,\lambda^5 + (J_{11}\,J_{33} + J_{11}\,J_{44} + J_{11}\,J_{55} + J_{11}\,J_{66} - J_{12}\,J_{21} \\ & -J_{13}\,J_{31} + J_{33}\,J_{44} + J_{33}\,J_{55} + J_{33}\,J_{66} + J_{44}\,J_{55} + J_{44}\,J_{66} + J_{55}\,J_{66})\lambda^4 + (-J_{11}\,J_{33}\,J_{44} \\ & -J_{11}\,J_{33}\,J_{55} - J_{11}\,J_{33}\,J_{66} - J_{11}\,J_{44}\,J_{55} - J_{11}\,J_{44}\,J_{66} - J_{11}\,J_{55}\,J_{66} + J_{12}\,J_{21}\,J_{33} + \\ & J_{12}\,J_{21}\,J_{44} + J_{12}\,J_{21}\,J_{55} + J_{12}\,J_{21}\,J_{66} - J_{13}\,J_{21}\,J_{32} + J_{13}\,J_{31}\,J_{44} + J_{13}\,J_{31}\,J_{55} + \\ & J_{13}\,J_{31}\,J_{66} - J_{33}\,J_{44}\,J_{55} - J_{33}\,J_{44}\,J_{66} - J_{33}\,J_{55}\,J_{66} - J - 44\,J_{55}\,J_{66})\lambda^3 + (J_{11}\,J_{33}\,J_{44}\,J_{55} \\ & +J_{11}\,J_{33}\,J_{44}\,J_{66} + J_{11}\,J_{33}\,J_{55}\,J_{66} + J_{11}\,J_{44}\,J_{55}\,J_{66} - J_{12}\,J_{21}\,J_{33}\,J_{44} - J_{12}\,J_{21}\,J_{33}\,J_{55} - \\ & J_{12}\,J_{21}\,J_{33}\,J_{66} - J_{12}\,J_{21}\,J_{44}\,J_{55} - J_{12}\,J_{21}\,J_{44}\,J_{66} - J_{12}\,J_{21}\,J_{55}\,J_{66} + J_{13}\,J_{21}\,J_{32}\,J_{44} + \\ & J_{13}\,J_{21}\,J_{32}\,J_{55} + J_{13}\,J_{21}\,J_{32}\,J_{66} - J_{13}\,J_{31}\,J_{44}\,J_{55} - J_{13}\,J_{31}\,J_{44}\,J_{66} - J_{13}\,J_{31}\,J_{55}\,J_{66} + \\ & J_{33}\,J_{44}\,J_{55}\,J_{66})\lambda^2 + (-J_{11}\,J_{33}\,J_{44}\,J_{55}\,J_{66} + J_{12}\,J_{21}\,J_{33}\,J_{44}\,J_{55} + J_{12}\,J_{21}\,J_{33}\,J_{44}\,J_{66} + \\ & J_{12}\,J_{21}\,J_{33}\,J_{55}\,J_{66} + J_{12}\,J_{21}\,J_{44}\,J_{55}\,J_{66} - J_{13}\,J_{21}\,J_{32}\,J_{44}\,J_{55} - J_{13}\,J_{21}\,J_{32}\,J_{44}\,J_{66} - \\ & J_{13}\,J_{21}\,J_{32}\,J_{55}\,J_{66} + J_{13}\,J_{31}\,J_{44}\,J_{55}\,J_{66})\lambda - J_{66}\,J_{55}\,J_{44}\,J_{21}\,(J_{12}\,J_{33} - J_{13}\,J_{32}) \end{cases} \tag{2.7}$$

3.0 Bifurcation and Hysteresis Effects of COVID-19 Model

In this section, a center manifold theory is applied to unfold the bifurcation behaviour of the model in system 1.2 around the disease free equilibrium E0 and endemic equilibrium point E1. This established the local stability of a non-hyperbolic equilibrium emanated from the centre manifold, and existence of another equilibrium, bifurcated from the non-hyperbolic equilibrium.

3.1 Centre Manifold Dynamics in COVID-19 Model

Theorem 4[[4]] Consider a general system of ordinary differential equation with parameter ϕ in closed form as:

$$\frac{dX}{dt} = F(X,\phi),\ F : R^n \times R \to R\ \ and\ \ F \in C^2(R^n \times R) \tag{2.8}$$

WLG, it is assumed that 0 is an equilibrium point of the system **??**2.8) $\forall$ values of the parameter ϕ such that $F(0,\phi) = 0$. Similarly, assume that

- $A = D_X F_i(0,0) = \left(\frac{\partial F}{\partial X_i}\right)(0,0)$ is the linearization matrix of system 2.8 around the equilibrium 0 with *phi* evaluated at 0. Zero being the simple eigenvalue of the matrix A, and all other eigenvalues of A have negative real parts.
- Matrix A has a non-negative right eigenvector w and a left eigenvector v corresponding to the eigenvalue.
  Let F_k be the kth component of F and

$$\begin{cases} a = \sum\limits_{k,i,j=1}^{n} v_k w_i w_j \left(\frac{\partial^2 F_k}{\partial X_i \partial X_j}\right)(0,0) \\ b = \sum\limits_{k,i,j=1}^{n} v_k w_i \left(\frac{\partial^2 F_k}{\partial X_i \partial \phi}\right)(0,0) \end{cases} \tag{2.9}$$

The local dynamics of system **??** around zero(0) are totally determined by a and b as follows:

i $a > 0$, $b > 0$. When $\phi < 0$ with $|\phi \ll 1|$, 0 is locally asymptotically stable, and there exists a positive unstable equilibrium; when $0 < \phi \ll 1$, 0 is unstable and there exists a negative and locally asymptotically stable equilibrium.

ii $a < 0$, $b > 0$. When $\phi < 0$ with $|\phi \ll 1|$, 0 is unstable; when $0 < \phi \ll 1$, 0 is locally asymptotically stable, and positive unstable equilibrium appears.

iii $a > 0$, $b < 0$. When $\phi < 0$ with $|\phi \ll 1|$, 0 is unstable, and there exists a locally asymptotically stable negative equilibrium; when $0 < \phi \ll 1$, 0 is locally asymptotically stable, and positive unstable equilibrium appears.

iv $a < 0$, $b > 0$. When ϕ changes from negative to positive, 0 changes its stability from stable to unstable. Correspondingly a negative equilibrium becomes positive and locally asymptotically stable.

Remark When $a > 0, b > 0$, the bifurcation at ϕ is sub-critical(backward) with hysteresis effect. The non-negativity of components of the eigenvector w is not necessary if corresponding component of equilibrium.

3.2 Eigenvalue and Eigenvector Analysis at the Centre Manifold

Theorem 4 can be applied to model of system 1.2 be taking the state variable as components of vector$X_i = (S, E, I, A, H, R)^T \cong (x_1, x_2, x_3, x_4, x_5, x_6)^T$. In this model the quasi-lockdown parameter κ, which controls the influx of susceptible class to transmission and transition of the infection in the mixed of entire population is the bifurcation paramter. This lockdown parameter begins to control the dynamics of the model as the disease start spreading, more or less when the basic reproduction number $R_0 \leq 1$. This dynamics can be visualized when evaluating the Jacobian matrix in system 2.5 at the disease free equilibrium point E_0. In this case the bifurcation parameter κ yields a simple

zero eigenvalue and the corresponding right and left eigenvectors defined as follows.

$$\begin{cases} & R_0 = 1, \kappa^* = \frac{\rho\varepsilon+\sigma+\varrho-\varepsilon}{\beta(\alpha-\sigma)} \\ & w = \left[w_1 = \frac{a_1}{a_2} \;\; w_2 = \frac{b_1}{b_2} \;\; w_3 = \frac{c_1}{c_2} \;\; w_4 = \frac{d_1}{d_2} \;\; w_5 = \frac{c_1}{c_2}, \;\; w_6 = 1\right]^T \\ & v = [v_1 = 0 \; v_2 = 1 \; v_3 = 0 \; v_4 = 0 \; v_5 = 0 \; v_6 = 0]^T \\ where & \\ a_1 = & -(\rho\,\varepsilon + \sigma + \varrho - \varepsilon)\,(\delta + \sigma + \upsilon)\;(\eta + \omega + \sigma)\,(\xi + \sigma)\,(\beta\,\psi + \beta\,\sigma + \beta\,\varsigma - \mu\,\sigma - \mu\,\varrho + \mu\,\varepsilon) \\ a_2 = & (-\delta\,\eta\,\mu\,\rho^2\varepsilon - \delta\,\mu\,\omega\,\rho^2\varepsilon - \delta\,\mu\,\rho^2\sigma\,\varepsilon + 2\,\beta\,\delta\,\eta\,\psi\,\rho + \beta\,\delta\,\eta\,\rho\,\sigma + \beta\,\delta\,\eta\,\rho\,\varsigma + \beta\,\delta\,\omega\,\psi\,\rho + \beta\,\delta\,\omega\,\rho\,\sigma \\ & +\beta\,\delta\,\omega\,\rho\,\varsigma + \beta\,\delta\,\psi\,\rho\,\sigma + \beta\,\delta\,\rho\,\sigma^2 + \beta\,\delta\,\rho\,\sigma\,\varsigma + \beta\,\eta\,\psi\,\rho\,\sigma + \beta\,\eta\,\psi\,\rho\,\upsilon - \delta\,\eta\,\mu\,\rho\,\sigma - \delta\,\eta\,\mu\,\rho\,\varrho \\ & +2\,\delta\,\eta\,\mu\,\rho\,\varepsilon - \delta\,\mu\,\omega\,\rho\,\sigma - \delta\,\mu\,\omega\,\rho\,\varrho + 2\,\delta\,\mu\,\omega\,\rho\,\varepsilon - \delta\,\mu\,\rho\,\sigma^2 - \delta\,\mu\,\rho\,\sigma\,\varrho + 2\,\delta\,\mu\,\rho\,\sigma\,\varepsilon - \beta\,\delta\,\eta\,\psi \\ & -\beta\,\delta\,\eta\,\sigma - \beta\,\delta\,\eta\,\varsigma - \beta\,\delta\,\omega\,\psi - \beta\,\delta\,\omega\,\sigma - \beta\,\delta\,\omega\,\varsigma - \beta\,\delta\,\psi\,\sigma - \beta\,\delta\,\sigma^2 - \beta\,\delta\,\sigma\,\varsigma + \delta\,\eta\,\mu\,\sigma + \\ & \delta\,\eta\,\mu\,\varrho - \delta\,\eta\,\mu\,\varepsilon + \delta\,\mu\,\omega\,\sigma + \delta\,\mu\,\omega\,\varrho - \delta\,\mu\,\omega\,\varepsilon + \delta\,\mu\,\sigma^2 + \delta\,\mu\,\sigma\,\varrho - \delta\,\mu\,\sigma\,\varepsilon)\varepsilon\;(\alpha - \sigma) \\ b_1 = & (-\mu\,\rho\,\varepsilon + \beta\,\psi + \beta\,\sigma + \beta\,\varsigma - \mu\,\sigma - \mu\,\varrho + \mu\,\varepsilon)\,(\delta + \sigma + \upsilon)\,(\eta + \omega + \sigma)\,(\xi + \sigma) \\ b_2 = & (-\delta\,\eta\,\mu\,\rho^2\varepsilon - \delta\,\mu\,\omega\,\rho^2\varepsilon - \delta\,\mu\,\rho^2\sigma\,\varepsilon + 2\,\beta\,\delta\,\eta\,\psi\,\rho + \beta\,\delta\,\eta\,\rho\,\sigma + \beta\,\delta\,\eta\,\rho\,\varsigma + \beta\,\delta\,\omega\,\psi\,\rho + \beta\,\delta\,\omega\,\rho\,\sigma \\ & +\beta\,\delta\,\omega\,\rho\,\varsigma + \beta\,\delta\,\psi\,\rho\,\sigma + \beta\,\delta\,\rho\,\sigma^2 + \beta\,\delta\,\rho\,\sigma\,\varsigma + \beta\,\eta\,\psi\,\rho\,\sigma + \beta\,\eta\,\psi\,\rho\,\upsilon - \delta\,\eta\,\mu\,\rho\,\sigma - \delta\,\eta\,\mu\,\rho\,\varrho \\ & +2\,\delta\,\eta\,\mu\,\rho\,\varepsilon - \delta\,\mu\,\omega\,\rho\,\sigma - \delta\,\mu\,\omega\,\rho\,\varrho + 2\,\delta\,\mu\,\omega\,\rho\,\varepsilon - \delta\,\mu\,\rho\,\sigma^2 - \delta\,\mu\,\rho\,\sigma\,\varrho + 2\,\delta\,\mu\,\rho\,\sigma\,\varepsilon - \beta\,\delta\,\eta\,\psi \\ & -\beta\,\delta\,\eta\,\sigma - \beta\,\delta\,\eta\,\varsigma - \beta\,\delta\,\omega\,\psi - \beta\,\delta\,\omega\,\sigma - \beta\,\delta\,\omega\,\varsigma - \beta\,\delta\,\psi\,\sigma - \beta\,\delta\,\sigma^2 - \beta\,\delta\,\sigma\,\varsigma + \delta\,\eta\,\mu\,\sigma + \\ & \delta\,\eta\,\mu\,\varrho - \delta\,\eta\,\mu\,\varepsilon + \delta\,\mu\,\omega\,\sigma + \delta\,\mu\,\omega\,\varrho - \delta\,\mu\,\omega\,\varepsilon + \delta\,\mu\,\sigma^2 + \delta\,\mu\,\sigma\,\varrho - \delta\,\mu\,\sigma\,\varepsilon)\varepsilon \\ c_1 = & \beta\rho(\delta + \sigma + \nu)(\eta + \omega + \sigma)(\xi + \sigma) \\ c_2 = & (-\delta\,\eta\,\mu\,\rho^2\varepsilon - \delta\,\mu\,\omega\,\rho^2\varepsilon - \delta\,\mu\,\rho^2\sigma\,\varepsilon + 2\,\beta\,\delta\,\eta\,\psi\,\rho + \beta\,\delta\,\eta\,\rho\,\sigma + \beta\,\delta\,\eta\,\rho\,\varsigma + \beta\,\delta\,\omega\,\psi\,\rho + \beta\,\delta\,\omega\,\rho\,\sigma \\ & +\beta\,\delta\,\omega\,\rho\,\varsigma + \beta\,\delta\,\psi\,\rho\,\sigma + \beta\,\delta\,\rho\,\sigma^2 + \beta\,\delta\,\rho\,\sigma\,\varsigma + \beta\,\eta\,\psi\,\rho\,\sigma + \beta\,\eta\,\psi\,\rho\,\upsilon - \delta\,\eta\,\mu\,\rho\,\sigma - \delta\,\eta\,\mu\,\rho\,\varrho \\ & +2\,\delta\,\eta\,\mu\,\rho\,\varepsilon - \delta\,\mu\,\omega\,\rho\,\sigma - \delta\,\mu\,\omega\,\rho\,\varrho + 2\,\delta\,\mu\,\omega\,\rho\,\varepsilon - \delta\,\mu\,\rho\,\sigma^2 - \delta\,\mu\,\rho\,\sigma\,\varrho + 2\,\delta\,\mu\,\rho\,\sigma\,\varepsilon - \beta\,\delta\,\eta\,\psi \\ & -\beta\,\delta\,\eta\,\sigma - \beta\,\delta\,\eta\,\varsigma - \beta\,\delta\,\omega\,\psi - \beta\,\delta\,\omega\,\sigma - \beta\,\delta\,\omega\,\varsigma - \beta\,\delta\,\psi\,\sigma - \beta\,\delta\,\sigma^2 - \beta\,\delta\,\sigma\,\varsigma + \delta\,\eta\,\mu\,\sigma + \\ & \delta\,\eta\,\mu\,\varrho - \delta\,\eta\,\mu\,\varepsilon + \delta\,\mu\,\omega\,\sigma + \delta\,\mu\,\omega\,\varrho - \delta\,\mu\,\omega\,\varepsilon + \delta\,\mu\,\sigma^2 + \delta\,\mu\,\sigma\,\varrho - \delta\,\mu\,\sigma\,\varepsilon) \\ d_1 = & (\eta + \omega + \sigma)\,(\xi + \sigma)\,(\rho - 1)\,(-\mu\,\rho\,\varepsilon + \beta\,\psi + \beta\,\sigma + \beta\,\varsigma - \mu\,\sigma - \mu\,\varrho + \mu\,\varepsilon)' \quad d_2 = c_2 \\ e_1 = & \phi\rho\beta(\xi + \sigma)(\delta + \sigma + \nu), \quad e_2 = d_2 \end{cases} \tag{2.9}$$

The bifurcation coefficients a and b, at the centre manifold are computed using the non-negative left and right eigenvectors of system 2.9. Also, the nonzero second order partial derivatives of the state variables, when evaluated using the quasi-locklown measure(bifurcation parameter), determines the direction of bifurcation. This simplifies the bifurcation coefficient at the centre manifold with effect of quasi-lockdown policy as follows;

$$\begin{cases} a = 2v_2w_1w_2\frac{\partial^2 f_2(\kappa^*)}{\partial x_1 \partial x_2} = 2v_2w_1w_2\kappa^* = 2v_2w_1w_2\frac{\rho\varepsilon+\sigma+\varrho-\varepsilon}{\beta(\alpha-\sigma)} < 0, \;\; \alpha < \sigma < \varepsilon(1-\rho) + \varrho \\ b = v_2w_1\frac{\partial^2 f_2(\kappa^*)}{\partial x_1 \partial \kappa^*} + v_2w_2\frac{\partial^2 f_2(\kappa^*)}{\partial x_1 \partial \kappa^*} = 2v_2\kappa^*(w_1 + w_2) = 2v_2(w_1 + w_2)\frac{\rho\varepsilon+\sigma+\varrho-\varepsilon}{\beta(\alpha-\sigma)} > 0, \\ where \\ \alpha < \sigma < \varepsilon(1-\rho) + \varrho \end{cases} \tag{3.0}$$

Observe that the computed coefficient of bifurcation changes sign at the speed determine by quantity $\alpha < \sigma < \varepsilon(1-\rho) + \varrho$. Hence, the centre manifold theory depicts the existence of forward and transcritical bifurcation with forward hysteresis effects. Epidemiologically, the quasi-lockdown policy necessitated reduction in the sporadic spread of the disease, but not sufficient to extinct the virus from the system. This implies that restrictions such as schools closure, halting of major organizational gatherings (church and mosques), stoppage of clusters in market places and shutting down business premises had curtail the spread of the infection, although the disease could persist endemically.

4.0 Computational Dynamics and Numerical Simulations in the Model

This section discussed data analytic in the model with the help of simulation packages in maple16.

4.1 Estimation of Epidemiologic datasets using Nonlinear Regression Model

The observed dataset from NCDC are parameterized and fitted using nonlinear least Square regression for predictive and simulation purposes. The NLS regression model y = f(x) for a ten point datasets($n = 10$), were used to estimate unknown epidemiologic parameters Θ_i, which minimizing the values of the differences between the sum of squares of the observed datasets , and the fitted data ($y = f(x_i)$ as such that,

$$min\Theta_i = \sum_{i,j=1}^{n} [y_i - f(x_j)] \tag{3.1a}$$

$$R^2 = 1 - \frac{\sum\limits_{i=1^n} (y_i - \bar{y})^2}{\sum\limits_{i=1}^{2} y_i^2 - \frac{\sum\limits_{i=1}^{n} y_i^2}{n\left(\sum\limits_{i=1}^{n} y_i\right)^2}} \tag{3.1b}$$

$$f(x^*) \pm t_{\frac{\alpha}{2}} \frac{s}{\sqrt{n}} \left(1 + \frac{1}{n} + \frac{(x^* - \bar{x})}{\sum\limits_{i=1}^{n} (x_i - \bar{x})^2} \right), \quad \forall x^* \in x_i \tag{3.1c}$$

The least square minimizing function is given equation 3.1a, coefficient of determination is given in 3.1b, and equation 3.1c depicts the predictable interval of the datasets within a 95% credibility at 0.05 level of significance. Its necessary to envisage that the closer the coefficient of determination R^2 to 1, the better the fitted datasets into the observed datasets. Table 1 reveals the observed datasetS, percliar to Akwa Ibom State as reported by NCDC. Its specifies the epic-weeks of the infection, weekly datasets, cumulative confirmed cases (CCC), recovery cases (RC), death case (RC), active active(AC), case fatility ratio (CFR), case recovery ratio (CRR) as seen in table 1.

Table 1 Weekly Report of COVID-19 from NCDC for Akwa Ibom (NCDC, 2023)

August, 2021	Weeks	CCC	RC	DC	AC	CFR	CRR
9th to 15th August, 2021	32	3511	2650	32	829	0.911421248	0.754770721
16th to 22nd August, 2021	33	3739	2943	32	764	0.855843809	0.787108853
23rd to 29th August, 2021	34	3984	3200	42	742	1.054216867	0.803212851
30th Aug., to 5th Sept, 2021	35	4135	3355	42	738	1.015719468	0.811366385
6th to 12th Sept, 2021	36	4221	3534	42	645	0.995024876	0.83724236
13th to 19th Sept, 2021	37	4282	3647	42	593	0.98085007	0.851704811
20th to 26th Sept, 2021	38	4319	3714	42	563	0.972447326	0.859921278
27th Sept, to 3rd Oct, 2021	39	4335	3864	44	427	1.014994233	0.891349481
4th to 10th Oct, 2021	40	4342	3940	44	358	1.0133579	0.907415937
11th to 17th Oct, 2021	41	4346	3986	44	316	1.012425219	0.917165209

According to the Nigeria Centre of Disease Control ([NCDC], 2023), the spread of the infection was in its epic-week within 1st to 30th August, 2021. The dataset extracted within this time frame is shown in table 1, and were used for fitting parameters and estimation of state variable in the model. There are relatively good line of best fits as shown in figure 3. Figure 3 has relatively high

coefficient of determination; $R^2 = 0.94$ on average. Using the regression model, the average fatality rate and recovery rate of the infection were fitted as 0.98% and 0.84% respectively. This implies a low recovery rate and less than 1% chance of surviving after contacting the virus. The estimated

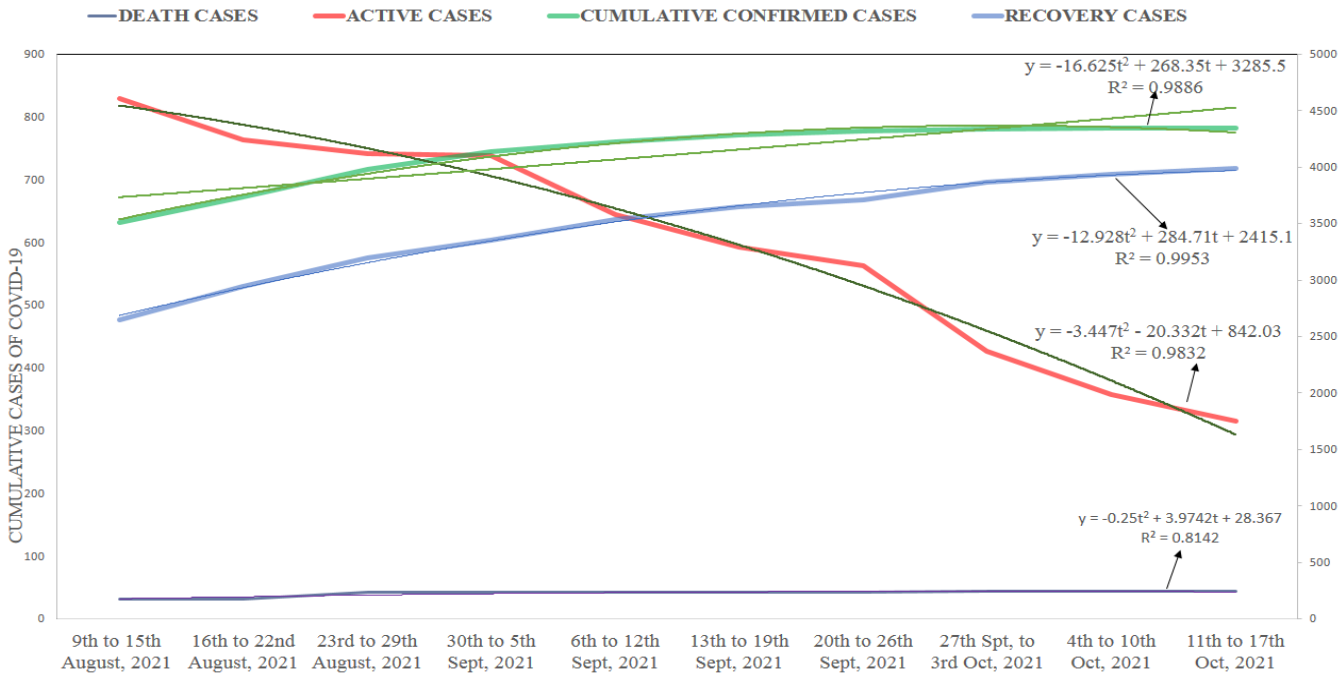

Figure 3: Lines of best fit of cases of COVID-19 in Epic-Weeks in Akwa Ibom (NCDC, 2023)

parameter values associated with 95% prediction intervals for compartmental population yields the result in table 2. Using the total population of people (National Bureau of Statistics [NBS], 2018) in Akwa Ibom state $4,987,740$ people, and before the quasi-lockdown policy, the susceptible population was estimated. The total intrinsic growth rate and recruitment of people into the susceptible class depends on the natural birth rate per woman per year in the entire population. Using the birth registration data $157,121$ in 2016, the natural birth rate and recruitment to the susceptible class, $\alpha = \frac{157121}{4987740} \times 100 = 4.15\%$. Since the estimated incubation period of the infection is between 13 days to 15 days, the effective progression rate ρ on average from exposed class to infected class is estimated as $\rho = \frac{1}{5.21 \times 14}$ per week. The average death rates in respective compartments, as well as the recovery rates are estimated within the interval $(0, 3]$ respectively. The natural death rates are equal in each compartment, and estimated using the life-expectancy. The life expectancy of adults individuals in Akwa Ibom state is approximated 52.1years, hence the natural death rate $\sigma = \frac{1}{52.11 \times 72}$ per week. On restrictions due to quasi-lockdown policy, the paramter κ is free and uncertain. Other parameters are estimated using validated results from the literature as see in table 2 below.

Table 2: Parameterization of COVID-19 epidemiologic variables

Meaning	Notations	Estimated values	RC Source
Susceptible class	$S(t_0)$	4.9×10^6	fitted
Exposed class	$E(t_0)$	***	estimated
Infected class	$I(t_0)$	3286	fitted
Asymptomatic infected class	$A(t_0)$	***	estimated
Hospitalized class	$H(t_0)$	842	fitted
Recovered class	$R(t_0)$	2415	fitted
Natural birth rate	α	10.5	estimated
Transmission rate from susceptible to exposed	β	1.75	estimated
Transmission rate from susceptible to infected	μ	1×10^{-6}	estimated
Transition rate from exposed to asymptomatic	ε	0.5	esitmated
Proportion of exposed that moved to infected	ρ	1.98	estimated
Transition rate from hospitalized to recovery	η	1.50	estimated
Recovery rate from asymotomatic(yeld immunity)	δ	1.5	estimated
Natural death rate	σ	0.02	estimated
Disease induced death rate of hospitalized	ω	2.5	estimated
Disease induced death rate of Asymptomatic	ν	1.22	estimated
Disease induced death rate of infected	ς	0.2235	estimated
Disease induced death rate of exposed	ϱ	2.005	estimated
Uncertain death rate after recovery	ξ	0.5	estimated
Quasi-lockdown measure	κ	$(0, \infty]$	controller

4.2 Sensitivity Analysis of Basic Reproduction(R_0)

A Normalized Forward Sensitivity Index(NFCI) is required to establish the computational fidelity of the model. Uncertainties, and effective changes of epidemiological parameters against the spread of the infection(basic reproduction number; R_0), and quasi-lockdown effect (κ) can be comptuted using NFCI. Consider a response function $R_0 = (F(X_p, p))$, where X_p is a parameter space, in respect to the parameter p, then the ratio of the relative changes in the response variable to the relative changes in the parameters, denoted as $S_p^{R_0} = \frac{\partial F}{\partial p}\frac{p}{R_0}$ defines the NFCI. In system of eqn 2.3, the basic reproduction number depends on parameters $(X_p = \beta, \alpha, \rho, \epsilon, \varepsilon, \sigma, \varrho)$. Applying this definition, the following indices were obtained, dependent on the basic reproduction number(R_0). Using table 3, the sign change of each sensitivity index predicts the direction of increase or decrease in the spread of the infection, dependent on parameter of interest. Clearly, table 3 shows that the quasi-lockdown policy(κ), and transition rate of susceptible to exposed class (β) yielded a significantly large effect size on the basic reproduction number(R_0) of the infection.

Table 3: Sensitive Indices of COVID-19 Parameters

Epidemiologic meaning	Paramters	Values	Sensitivity Indices
Natural birth rate	α	10.5	+0.001156
Natural death rate	σ	0.02	−0.0299
Transmission rate from susceptible to exposed	β	1.75	+1.0000
Transition rate from exposed to infected	ε	2.5	−0.6748
Proportion of exposed that moved to infected class	ρ	1.98	−1.3634
Disease induced death rate of exposed	ϱ	2.005	−0.3068
Quasi-lockdown measure(susceptibility capacity)	κ	3.77745	+1.0000

Figure 4 demonstrated a proportional increase in the spread of the infection, due to increase of influx of people by birth $\alpha = +ve$ to the susceptible class, and increase in the transmission rate $\beta = +ve$ from susceptible to exposed class. This implies that an increase of 10% of people by birth to the susceptible class will leads to an increase in 0.02% in the basic reproduction number

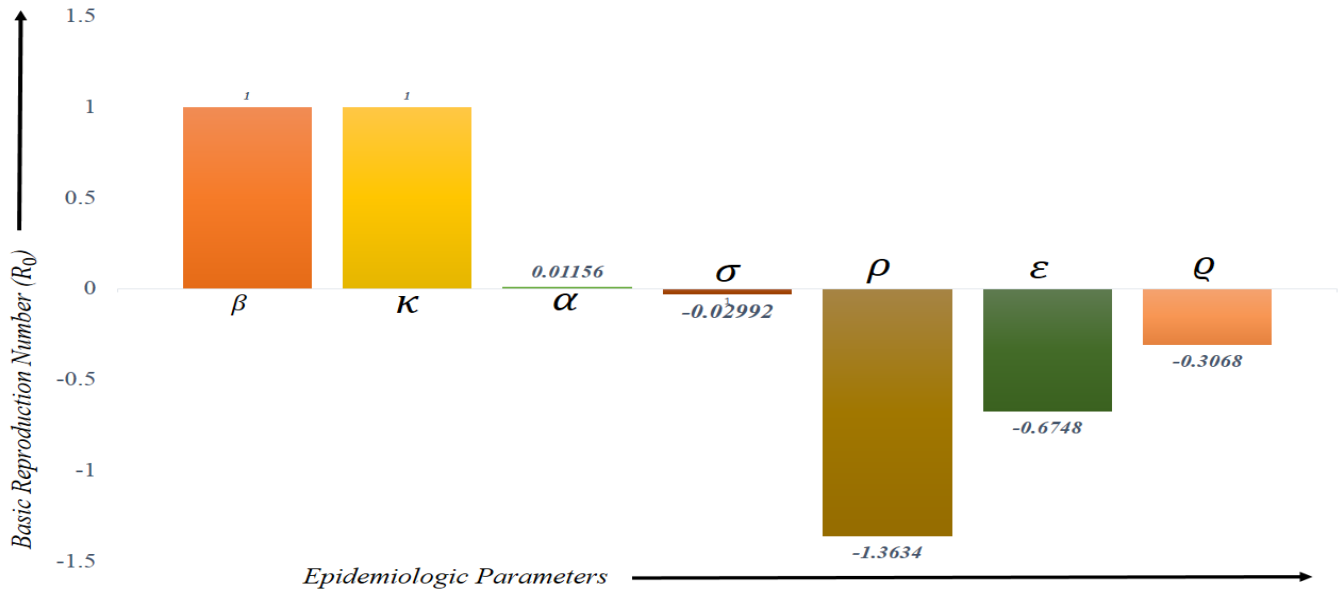

Figure 4: Tornado plot profile of COVID-19 sensitivity indices in Akwa Ibom State

R_0 of the infection. Similarly, an increase by 10% of the disease transmission rate to the exposed class, will leads to a corresponding increase in 10% of the basic reproduction number R_0 of the disease. Observe that, the quasi-lockdown measure $\kappa = +ve$ which signifies restriction movement of susceptible class, can possibly increase the spread of the infection, when more people are allowed to interact. Empirically, an increase in number of susceptible persons by relaxation of the quasi-lockdown measure by 10%, will leads to a corresponding increase of 10% in the basic reproduction number R_0 of the disease. Consequently, other parameters of the basic reproduction number indicate an increasing trend of the basic reproduction number, when they are decreased. A contour map and phase space diagram is used to visualized the dynamics of the basic reproduction numberR_0 plotted against other parameters.

4.3 Contour Maps of COVID-19 Basic Reproduction Number and Sensitive Parameters

Contour maps and phase space diagram has been used to visualize the dynamical interactions between the basic reproduction number; R_0, and some sensitive parameters. Figure 6(a-i) illustrates the changes in basic reproduction(R_0) as plotted against the transition rate of susceptible class(β) to the exposed classed, as well as the effectiveness of the quasi-lockdown measure(κ).

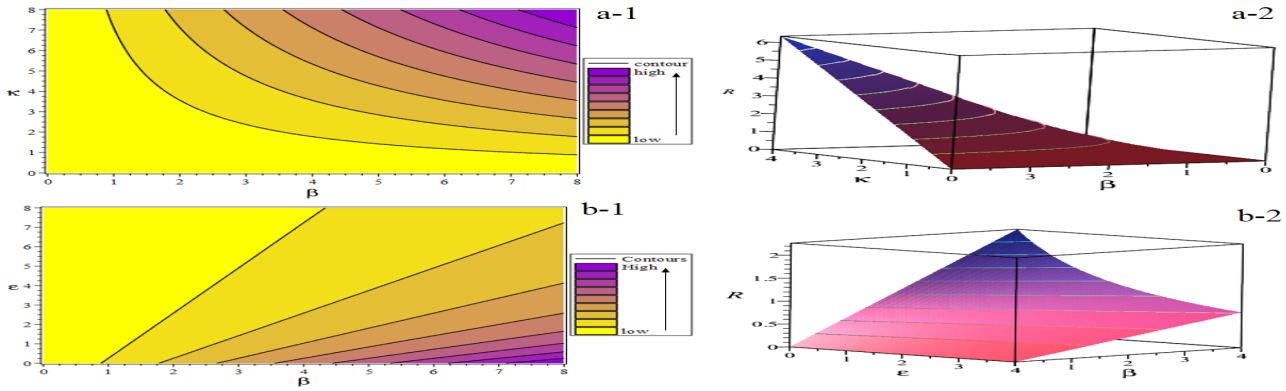

Figure 5: Contour and phase space diagram of R_0 against β , ε *and* κ

It shows that any increase in the population of the exposed class, increases the spread of the infection,and proportional increase in basic reproduction number (R_0). Its important to envisage that increasing the lockdown parameter implies increasing the susceptibility of the entire population to the disease. In figure 5(a-ii), relaxation of the lockdown policy or increasing the population of the susceptible class leads to a corresponding increase in the basic reproduction number(R_0). So, the partial lockdown policy assisted in curtailing the spread of the infection.

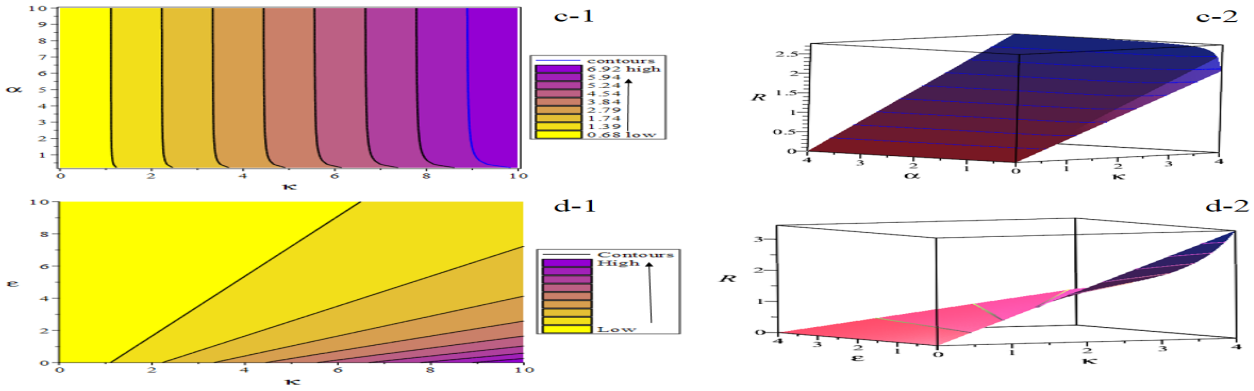

Figure 6: Contour and phase space diagram of R_0 against α, ε *and* κ

In Figure 5(b i and ii), the basic reproduction number is not sensitive to the transition rate of exposed to infected class, but sensitive to any increase in the infectivity of the susceptible class. Similar situation has been show in figure 6(c and d). This affirms the efficacy of restriction of susceptible class, through lockdown policy, as a major strategic to reduce the spread of the infection in the entire population.

4.4 Discussions of Dynamical Behaviours and Bifurcations at Equilibrium Points

Using the baseline epidemiologic datasets in table 2, the disease free equilibrium $E_0 \rightarrow (1.4829,\ 0,\ 0,\ 0,\ 0,\ 0)$, assumes asymptotically stable behaviour. This behaviour is possible when the quasi-lockdown policy $\kappa^* = 1.5$ was enforced strictly, and basic reproduction number $R_0 \leq 1$, $R_0^* = 0.3971 < 1$. This dynamics satisfies the conditions of theorem 4 since the characteristic polynomial;
$P(\lambda) = 250.2530 + 936.8059\lambda + 1219.9477\lambda^2 + 686.1668\lambda^3 + 183.9312\lambda^4 + 22.7435\lambda^5 + \lambda^6$,
yields negative eigenvalues;
$\lambda_1 = -3.94,\ \lambda_2 = -0.8435,\ \lambda_3 = -10.38,\ \lambda_5 = -2.84,\ \lambda_5 = -4.12,\ \lambda_6 = -0.620$
Hence the solution profile in figure 7, converges to a stable fixed point in the model.

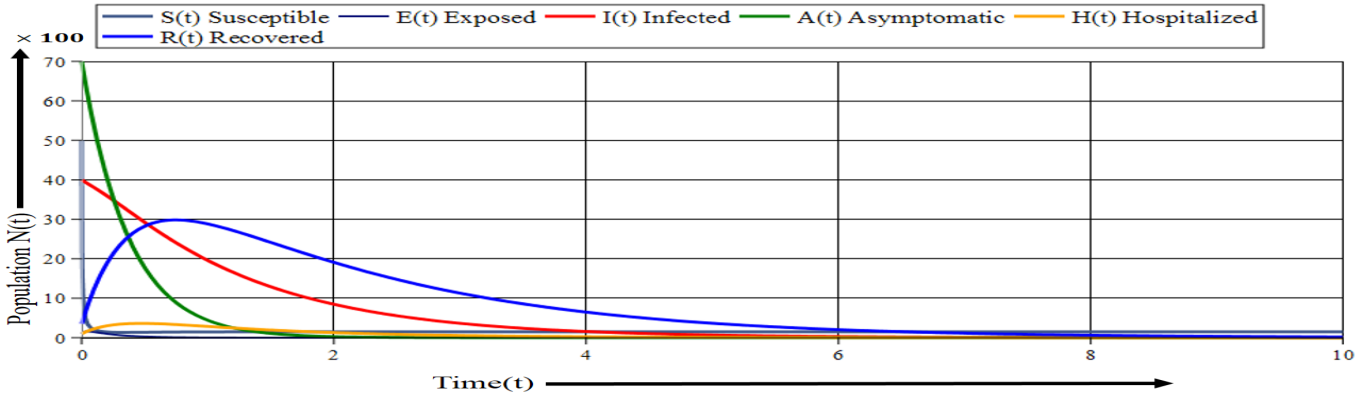

Figure 7: Stable dynamics at disease free equilibrium point

Similarly, the model remians stable at the disease free equilibrium on small relaxation of the quasi-lockdown policy κ, say $\kappa^* \in (0, 3.77745]$, with basic reproduction number $R_0 < 1$. Otherwise its bifurcates from the stable manifold at $R_0 = 1$, and degenerates a transcritical dynamics (see figure 8). This satisfies the conditions of existence of forward bifurcation with hysteresis effect[32, 24, 8], and conditions in theorem 4, where the bifurcation coefficients $a = -0.1836 < 0$, $b = 0.054 > 0$ changes sign. Accordingly, stable(red line), and unstable(blue) oscillating endemic region emerged from the stable transient bifurcation point. Also, the disease free equilibrium spans to the unstable region(yellow asymptote) as seen in figure 8 below.

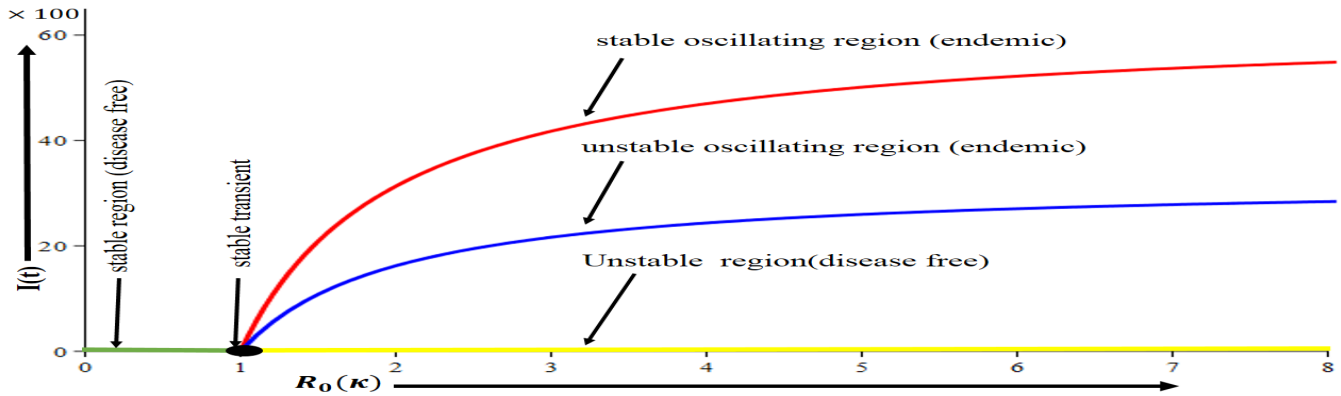

Figure 8: Diagram of forward and transcritical bifurcations at centre manifold $R_0 = 1$

These dynamics can be visualized using solution profiles at the endemic equilibrium points; stable and unstable oscillating solutions respectively. The oscillating solution converges to the stable endemic equilibrium point; $E_1 \to (S = 3.7343,\ E = 5.90898,\ I = 62.4185,\ A = 9.175575,\ H = 7.575062,\ R = 40.52574)$ as seen in figure 9.

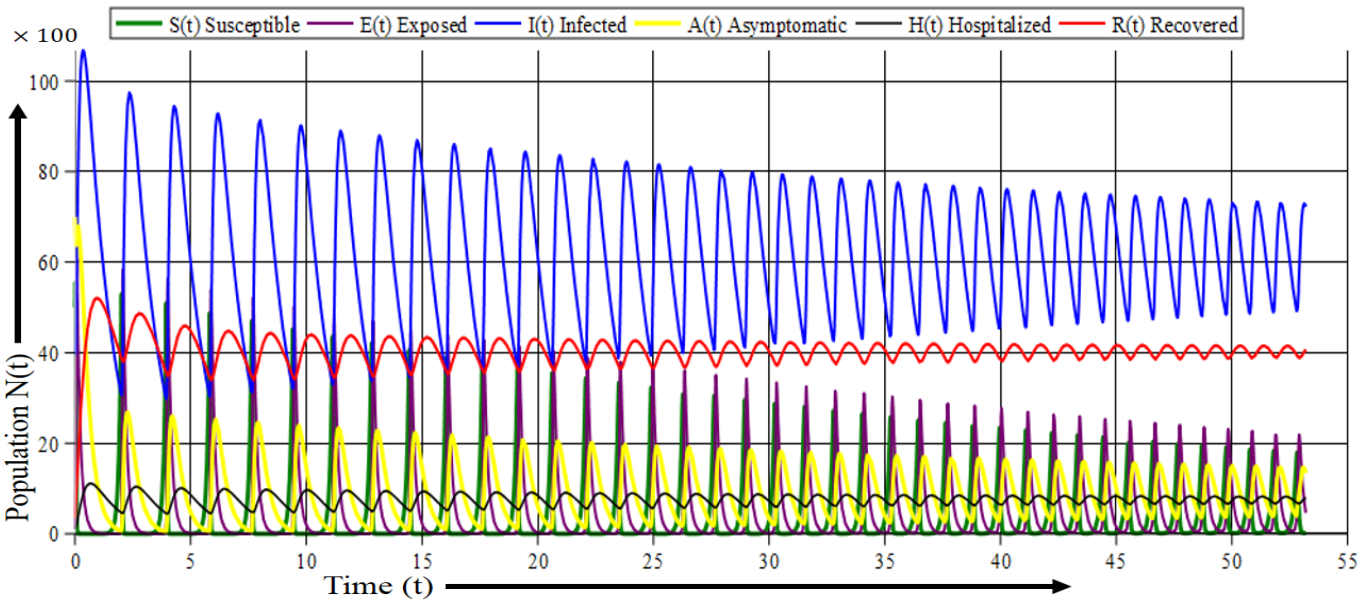

Figure 9: Stable oscillating solution profile at endemic equilibrium point (E_1)

These dynamics occur as the quasi-lockdowm measure was relaxed $(\kappa^* \in (3.77745, 1000])$, at the endemic equilibrium point $E_1 \to (S = 3.7343, E = 5.90898, I = 62.4185, A = 9.175575171, H = 7.57506, R = 40.52573634)$. The dynamics satisfies local stability conditions, as negative eigenvalues occurs when evaluating the characteristic polynomial;
$P(\lambda) = (-67.60972778\lambda - 0.8826949142\lambda^2 - \lambda^3 - 57.00023298)(-2.84 - \lambda)(-4.12 - \lambda)(-.62 - \lambda)$,
at the endemic equilibrium point. The oscillating solution occurs in accordance with theorem 3, when the basic reproduction number $R_0 > 1$, say $R_0 = 265 \in (1, \infty]$. Subsequently, a fur-

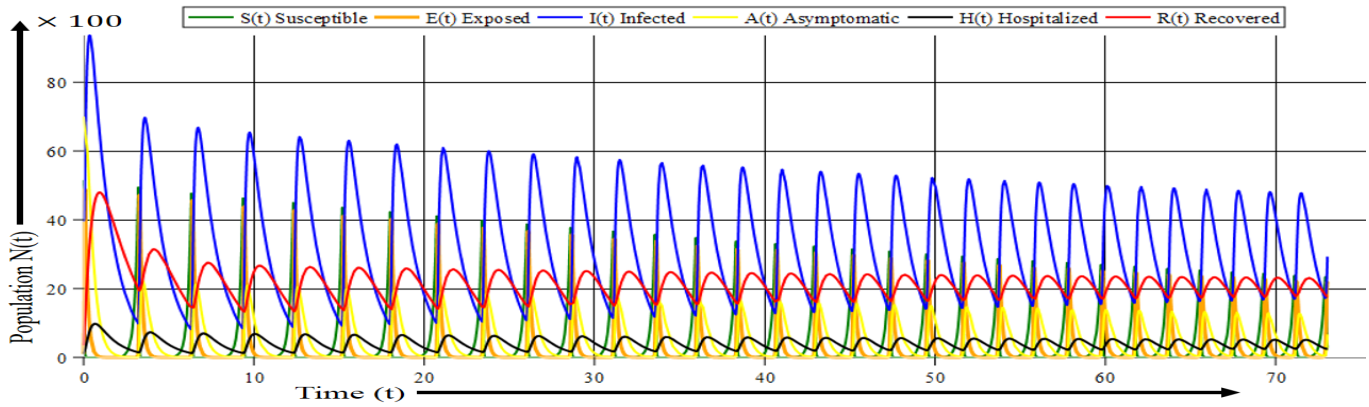

Figure 10: Unstable oscillating solution profile at endemic equilibrium point (E_1^*)

ther relaxation of the quasi-lockdown policy, say ($\kappa^* = 1000.15 \in (1000, \infty]$) yielded an unstable oscillating solution profile, which implies an existence of forward bifurcation with hysteresis effect(see figure 10). This oscillating dynamics is unstable at the endemic equilibrium point $E_1^* \to (S = 3.7342, E = 3.0625, I = 32.3505, A = 4.7555, H = 3.9260, R = 21.004)$, since at least one of the eigenvalues of the characteristic polynomial;
$P(\lambda) = 214.3144 - 19.0931\lambda^3 + 0.0308\lambda^4 - 84.657\lambda^2 - 2.2437 \times 10^{-9}\lambda^5 + \lambda^6 + 207.73492\lambda$,
given as $(2.6283 \pm 0.5997i,\ -0.7541 \pm 3.4331i,\ -2.93538,\ -0.8131)$ has a non negative real part. Epidemiologically, the model predicted a negative impacts in the state, if there was a further relaxation of the quasi-lockdown policy.

5.0 Conclusion

In this research work, a compartmental populations of susceptible, exposed, infected, asymptomatic, hospitalized and recovered(SEIAHR) model has been designed to describe the dynamics of COVID-19 pandemic in Akwa Ibom State. The model incorporates a logistic function, as the per capita influx rate of the entire population to the susceptible class, with the carrying capacity as a measure of quasi-lockdown policy. Its seeks to investigates the effectiveness of quasi-lockdown policy(a measure of strategic economy restrictions, and halting of human to human interactions of different forms) to curtail the spread of the infection in the state. The feasibility, well-possedness, existence and uniqueness of the model were established using fixed point theory. Qualitative dynamical behaviour of the model includes local stability of the pandemic free equilibrium, transcritical bifurcation, forward bifurcation with hysteresis effect(oscillating stable and unstable dynamics) as the disease persists endemically. The model demonstrated that the quasi-lockdown policy was necessarily effective to curtail the exponential spread of the infection in the population, when it was enforced strictly. On the other hand, the model predicted unstable oscillating behaviour when simulated using the baseline parameter, on variation and relaxation of the quasi-lockdown policy. Thus we envisaged that the quasi-lockdown policy was among the most effective for controlling virus development and spread, but a pre-mature lifting of the lockdown policy could have lead to disaster.

References

[1] E. T. Akpan, E. E Joshua, and E. I Uduk. Nonlinear dynamics and synchronization of computational cognitive model in educational sciences. *J. Nonlinear Sci. Appl*, 14(1):15–28, 2020.

[2] Joseph Bamidele Awotunde, Roseline Oluwaseun Ogundokun, Abidemi Emmanuel Adeniyi, Kazeem Moses Abiodun, and Gbemisola Janet Ajamu. Application of mathematical modelling approach in covid-19 transmission and interventions strategies. In *Modeling, Control and Drug Development for COVID-19 Outbreak Prevention*, pages 283–314. Springer, 2022.

[3] Fotini Boufidou, Snežana Medić, Vicky Lampropoulou, Nikolaos Siafakas, Athanasios Tsakris, and Cleo Anastassopoulou. Sars-cov-2 reinfections and long covid in the post-omicron phase of the pandemic. *International Journal of Molecular Sciences*, 24(16):12962, 2023.

[4] Carlos Castillo-Chavez and Baojun Song. Dynamical models of tuberculosis and their applications. *Math. Biosci. Eng*, 1(2):361–404, 2004.

[5] Pietro Cerone and Silvestru Sever Dragomir. *Mathematical inequalities: a perspective*. CRC Press, 2010.

[6] Marios Constantinou, Themis Exarchos, Aristidis G Vrahatis, and Panagiotis Vlamos. Covid-19 classification on chest x-ray images using deep learning methods. *International Journal of Environmental Research and Public Health*, 20(3):2035, 2023.

[7] Shasha Gao, Pant Binod, Chidozie Williams Chukwu, Theophilus Kwofie, Salman Safdar, Lora Newman, Seoyun Choe, Bimal Kumar Datta, Wisdom Kwame Attipoe, Wenjing Zhang, and P. van den Driessche. A mathematical model to assess the impact of testing and isolation compliance on the transmission of covid-19. *Infectious Disease Modelling*, 8(2):427–444, 2023.

[8] Jayanta Kumar Ghosh and Uttam Ghosh. Three dimensional epidemic model with non-monotonic incidence and saturated treatment: a case study of sars infection of hong kong 2003 scenario. *Results in Control and Optimization*, page 100239, 2023.

[9] Rutwik Gulakala, Bernd Markert, and Marcus Stoffel. Rapid diagnosis of covid-19 infections by a progressively growing gan and cnn optimisation. *Computer Methods and Programs in Biomedicine*, 229:107262, 2023.

[10] Morris W Hirsch, Stephen Smale, and Robert L Devaney. *Differential equations, dynamical systems, and an introduction to chaos*. Academic press, 2012.

[11] RH Huang, DJ Liu, J Guo, JF Yang, JH Zhao, XF Wei, S Knyazeva, M Li, RX Zhuang, CK Looi, et al. Guidance on flexible learning during campus closures: Ensuring course quality of higher education in covid-19 outbreak. *Beijing: Smart Learning Institute of Beijing Normal University*, 2020.

[12] Ronghuai Huang, DJ Liu, Ahmed Tlili, JunFeng Yang, HuaHaun Wang, et al. Handbook on facilitating flexible learning during educational disruption: The chinese experience in maintaining undisrupted learning in covid-19 outbreak. *Beijing: Smart Learning Institute of Beijing Normal University*, 46, 2020.

[13] Yoh Iwasa, Akane Hara, and Shihomi Ozone. Virulence of a virus: How it depends on growth rate, effectors, memory cells, and immune escape. *Journal of Theoretical Biology*, 530:110875, 2021.

[14] Sarbaz HA Khoshnaw, Kawther Yusuf Abdulrahman, and Arkan N Mustafa. Impact of vaccination strategies on the spread of covid-19 pandemics: A mathematical modelling approach. 2023.

[15] Zenebe Shiferaw Kifle and Legesse Lemecha Obsu. Co-dynamics of covid-19 and tb with covid-19 vaccination and exogenous reinfection for tb: An optimal control application. *Infectious Disease Modelling*, 8(2):574–602, 2023.

[16] L Kim, J Hayes, P Lewis, AV Parwani, KO Chang, and Linda Jean Saif. Molecular characterization and pathogenesis of transmissible gastroenteritis coronavirus (tgev) and porcine respiratory coronavirus (prcv) field isolates co-circulating in a swine herd. *Archives of virology*, 145:1133–1147, 2000.

[17] Manotosh Mandal, Soovoojeet Jana, Sayani Adak, Anupam Khatua, and Tapan Kumar Kar. A model-based analysis to predict and control the dynamics of covid-19. *Modeling, Control and Drug Development for COVID-19 Outbreak Prevention*, pages 87–118, 2022.

[18] Vimal K Maurya, Swatantra Kumar, Madan LB Bhatt, and Shailendra K Saxena. Therapeutic development and drugs for the treatment of covid-19. *Coronavirus Disease 2019 (COVID-19) Epidemiology, Pathogenesis, Diagnosis, and Therapeutics*, pages 109–126, 2020.

[19] M. Moss. The pandemic accord: Actualizing ambition in 2023. *Zdm*, 50(1):233–244, 2023.

[20] Mayowa M. Ojo, Olumuyiwa James Peter, Emile Franc Doungmo Goufo, and Kottakkaran Sooppy Nisar. A mathematical model for the co-dynamics of covid-19 and tuberculosis. *Mathematics and Computers in Simulation*, 207:499–520, 2023.

[21] S Olaniyi, OS Obabiyi, KO Okosun, AT Oladipo, and SO Adewale. Mathematical modelling and optimal cost-effective control of covid-19 transmission dynamics. *The European Physical Journal Plus*, 135(11):938, 2020.

[22] Paul Ani Onuh. Nigeria's response to covid-19: Lockdown policy and human rights violations. *African Security*, 14(4):439–459, 2021.

[23] World Health Organization et al. Novel coronavirus (2019-ncov): situation report, 11. 2020.

[24] Lawrence Perko. *Differential equations and dynamical systems*, volume 7. Springer Science & Business Media, 2013.

[25] Nicolas Reuge, Robert Jenkins, Matt Brossard, Bobby Soobrayan, Suguru Mizunoya, Jim Ackers, Linda Jones, and Wongani Grace Taulo. Education response to covid 19 pandemic, a special issue proposed by unicef: Editorial review. *International Journal of Educational Development*, 87:102485, 2021.

[26] Guoguang Rong, Yuqiao Zheng, Yin Chen, Yanjun Zhang, Peixi Zhu, and Mohamad Sawan. Covid-19 diagnostic methods and detection techniques. *Encyclopedia of sensors and biosensors*, page 17, 2023.

[27] Shikha Saha and Amit Kumar Saha. Modeling the dynamics of covid-19 in the presence of delta and omicron variants with vaccination and non-pharmaceutical interventions. *Heliyon*, 9(7), 2023.

[28] Shailendra K Saxena. *Coronavirus disease 2019 (COVID-19): epidemiology, pathogenesis, diagnosis, and therapeutics*. Springer nature, 2020.

[29] Nam K Tran, Samer Albahra, Hooman Rashidi, and Larissa May. Innovations in infectious disease testing: leveraging covid-19 pandemic technologies for the future. *Clinical Biochemistry*, 117:10–15, 2023.

[30] Nam K. Tran, Samer Albahra, Hooman Rashidi, and Larissa May. Innovations in infectious disease testing: Leveraging covid-19 pandemic technologies for the future. *Clinical Biochemistry*, 117:10–15, 2023. Innovations in Infectious Disease Diagnostics: Alternative Approaches and Near Patient Testing.

[31] Eleftheria Tzamali, Vangelis Sakkalis, Georgios Tzedakis, Emmanouil G Spanakis, and Nikos Tzanakis. Mathematical modeling evaluates how vaccinations affected the course of covid-19 disease progression. *Vaccines*, 11(4):722, 2023.

[32] Lin Zhang, Jiahua Zhu, Xuyuan Wang, Juan Yang, Xiao Fan Liu, and Xiao-Ke Xu. Characterizing covid-19 transmission: incubation period, reproduction rate, and multiple-generation spreading. *Frontiers in Physics*, 8:589963, 2021.